Stereoselective Oxidative Addition of Hydrogen to Iridium(I) Complexes. Kinetic Control Based on Ligand Electronic Effects

Curtis E. Johnson and Richard Eisenberg*

Contribution from the Department of Chemistry, University of Rochester, Rochester, New York 14627. *Received November 5, 1984*

Abstract: The oxidative addition of H_2 to the iridium(I) chelates $IrX(CO)(dppe)^{n+}$ (n = 0; X = Cl, Br, I, CN, H; n = 1, X = PPh_3; dppe = 1,2-bis(diphenylphosphino)ethane) proceeds with >99% stereoselectivity to yield a *cis*-dihydride product with one hydride trans to P(dppe) and the other hydride trans to CO. For X = Cl, Br, and I, the kinetic product of formula $IrH_2X(CO)(dppe)$ equilibrates with a more stable cis isomer which has one hydride trans to P and the other trans to X (K_{eq} = 41, 35, and 13, respectively). The stereochemical assignments based on chemical shifts of the hydride ligands are confirmed by single-crystal X-ray diffraction analysis of the thermodynamic isomer for X = Br. The complex $IrH_2Br(CO)(dppe)$ crystallizes in the orthorhombic space group $P2_12_12_1$ with unit cell parameters a = 12.291 (3) Å, b = 17.349 (4) Å, c = 12.189 (3) Å, V = 2599 Å^3, and Z = 4. The structure refined to a conventional R factor of 0.035. The isomerization reaction between the two dihydride isomers has been studied mechanistically in acetone and benzene solvents. In acetone, the isomerization of $IrH_2Br(CO)(dppe)$ proceeds with first-order kinetics in iridium complex (k = 0.011 min^{-1}), and the mechanism likely involves a two-step H_2 reductive elimination/oxidative addition process. For X = CN, the kinetic dihydride isomer is the most stable isomer, but it does thermally equilibrate with two other isomers. For X = H or PPh_3, only a single isomer is observed and it appears to be the most stable isomer. The stereoselectivity of D_2 oxidative addition for X = H is established by generating the reactive species IrH(CO)(dppe) in situ by dehydrohalogenation of $IrH_2Cl(CO)(dppe)$ under D_2. For all of the complexes studied, the stereochemistry of hydrogen oxidative addition is the same, and the observed stereoselectivity is dictated by electronic differences between the CO and X ligands. Possible explanations for the observed stereoselectivity are discussed in relation to current theories on the intimate mechanism of H_2 oxidative addition.

The activation of substrates via oxidative addition is a fundamental reaction in transition-metal chemistry and catalysis. In this context, the reaction of hydrogen with d^8 square-planar complexes has been extensively studied because of its central role in homogeneous hydrogenation and hydroformylation catalysis.[1] Historically, the reaction of hydrogen with *trans*-$IrCl(CO)(PPh_3)_2$, Vaska's complex, has come to be regarded as a prototype of the oxidative addition reaction of square-planar complexes.[2] This reaction, as shown in eq 1 for compounds of the general type *trans*-$IrX(CO)L_2$, is generally facile and reversible, making it convenient for mechanistic study.[3]

Several groups have investigated the mechanism of reaction 1, principally by determining kinetic and thermodynamic parameters as a function of the ligands X and L.[4] The generally accepted mechanism involves a concerted cis addition of H_2 along one of the ligand axes corresponding to a diagonal of the square complex, leading to formation of dihydride products with the stereochemistries shown via pathways i and ii in eq 1. In this oxidative addition, two primary interactions between the d^8 metal complex and the H_2 molecule occur. The first, shown as **A**, involves σ donation from the $\sigma^b(H_2)$ orbital into a vacant acceptor orbital on the metal center which is of p_z or p_z–d_{z^2} hybrid character. The second, **B**, is a back-bonding interaction in which electron density is transferred from a filled metal d orbital of π symmetry (either d_{xz} or d_{yz}) into the σ^* orbital of H_2. Both interactions serve to weaken the H–H bond while creating M–H bonds. As this concerted oxidative addition proceeds, one pair of trans ligands of the square-planar complex bends such that the product complex is octahedral with cis hydride ligands.

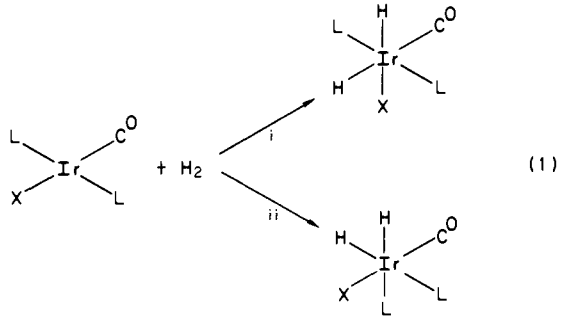

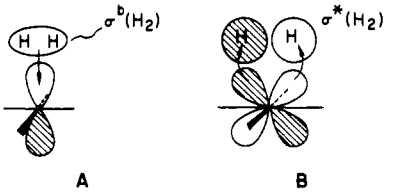

For H_2 oxidative addition with complexes of the type *trans*-$IrX(CO)L_2$, reactivity usually increases with increasing metal basicity. On the basis of kinetic and equilibrium data, and on changes in ν_{CO} of the Ir complex, Vaska views the addition of H_2 as oxidative in character with the back-bonding interaction **B** of primary importance.[4d] Crabtree, on the other hand, finds that electron-withdrawing ligands promote H_2 oxidative addition in

(1) (a) Collman, J. P.; Hegedus, L. S. "Principles and Applications of Organotransition Metal Chemistry"; University Science Books: Mill Valley, CA, 1980. (b) Parshall, G. W. "Homogeneous Catalysis"; Wiley: New York, 1980. (c) Cotton, F. A.; Wilkinson, G. "Advanced Inorganic Chemistry"; 4th ed.; Wiley: New York, 1980; Chapter 30.

(2) Vaska, L.; DiLuzio, J. W. *J. Am. Chem. Soc.* **1962**, *84*, 679–80.

(3) Two reviews by James cite most of the pertinent literature: (a) James, B. R. "Homogeneous Hydrogenation"; Wiley: New York, 1973; Chapter 12. (b) James, B. R. In "Comprehensive Organometallic Chemistry"; Wilkinson, G., Stone, F. G. A., Abel, E. W., Eds.; Pergamon Press: New York, 1982; Vol. 8, Chapter 51.

(4) (a) Chock, P. B.; Halpern, J. *J. Am. Chem. Soc.* **1966**, *88*, 3511–4. (b) Strohmeier, W.; Onada, T. *Z. Naturforsch.* **1968**, *23b*, 1527–8. (c) Strohmeier, W.; Muller, F. J. *Ibid.* **1969**, *24b*, 931–2. (d) Vaska, L.; Werneke, M. F. *Ann. N.Y. Acad. Sci.* **1971**, *172*, 546–62. (e) James, B. R.; Memon, N. A. *Can. J. Chem.* **1968**, *46*, 217–23. (f) Ugo, R.; Pasini, A.; Fusi, A.; Cenini, S. *J. Am. Chem. Soc.* **1972**, *94*, 7364–70. (g) Schmidt, R.; Geis, M.; Kelm, H. *Z. Phys. Chem. Neue Folge* **1974**, *92*, 223–34. (h) Hyde, E. M.; Shaw, B. L. *J. Chem. Soc., Dalton Trans.* **1975**, 765–7. (i) Blumer, D. J. Ph.D. Dissertation; University Microfilms International: Ann Arbor, MI, 1981.

0002-7863/85/1507-3148$01.50/0

Table I. IR and NMR Data of Ir(I) Compounds[a]

	ν_{CO}, cm^{-1}	^1H NMR δ_{CH_2}	$\delta_{o\text{-}C_6H_5}$[b]	$^{31}P\{^1H\}$ NMR
IrCl(CO)(dppe) (**1a**)	1983	2.80, 2.73, 2.45, 2.38	7.94 (4 H), 7.77 (4 H)	48.1, 43.3 (d, J = 13)
IrBr(CO)(dppe) (**1b**)	1986	2.75, 2.68, 2.43, 2.36	7.89 (4 H), 7.77 (4 H)	49.4, 45.1 (d, J = 13)
IrI(CO)(dppe) (**1c**)	1988	2.68, 2.61, 2.44, 2.37	7.84 (4 H), 7.78 (4 H)	50.7, 47.5 (d, J = 13)
Ir(CN)(CO)(dppe)[c] (**1d**)	1997	2.80, 2.73, 2.57, 2.50	7.96 (8 H)	51.9, 48.9 (d, J = 13)
$[Ir(PPh_3)(CO)(dppe)]NO_3$ (**1e**)	2008[g]			
$IrCl(CO)_2(dppe)$ (**2a**)	2035 (s), 1948 (s)[h]	2.91[i]	7.72 (8 H)	35.9 (s)
$IrBr(CO)_2(dppe)$ (**2b**)	2041 (s), 1950 (s)[h]	2.80[i]	7.73 (8 H)	36.9 (s)
$IrI(CO)_2(dppe)$ (**2c**)	2040 (s), 1950 (s)[h]	2.83[i]	7.72 (8 H)	33.8 (s)
$Ir(CN)(CO)_2(dppe)$[d] (**2d**)	2005 (m), 1960 (s)[h]	2.77[i]	7.74 (8 H)	27.4 (s)
$[Ir(PPh_3)(CO)_2(dppe)]NO$, (**2e**)	2010 (mw), 1965 (s)[g]	2.94[i]	7.56[j]	
$IrH(CO)_2(dppe)$[e] (**2g**)	1966, 1912	2.61[i]	7.71 (8 H)	33.8 (s)[k]
$PPN[Ir(CN)_2(CO)(dppe)]$[f] (**4**)	1900 (br)[g]	2.41[i]	7.84 (8 H)	23.3 (s)

[a] IR spectra are recorded from KBr pressed pellets, and ^1H NMR (400 MHz) and ^{31}P NMR (162 MHz) spectra are from acetone-d_6 solutions unless otherwise indicated. Couplings are in hertz. [b] The *o*-phenyl resonances of dppe are generally downfield of the corresponding meta and para resonances, and the assignments are confirmed by proton decoupling (J_P(ortho H) ~ 10 Hz). [c] ν_{CN} = 2118 (w) cm^{-1}. [d] ν_{CN} = 2140 (w) cm^{-1}. [e] ν_{IrH} = 2000 cm^{-1}. Some of the data are taken from ref 13. [f] ν_{CN} = 2094 (w) cm^{-1}. [g] Acetone solution. [h] THF solution. [i] Multiplet with intense inner doublet with a separation of 16–20 Hz. [j] The *m*- and *p*-phenyl dppe resonances overlap with the ortho resonance at δ 7.56. The peaks for PPh_3 are at δ 7.48, 7.35, and 7.09 for *p*-, *m*-, and *o*-Ph, respectively. [k] Benzene solution.

cationic iridium complexes of the type $Ir(diene)L_2^+$ and suggests that the reaction for these systems may be reductive to the metal center rather than oxidative.[5] Clearly, the influence of electronic properties of the ligands coordinated to the metal center on H_2 oxidative addition is not yet fully understood.[6]

In elucidating reaction mechanisms, the study of reaction stereochemistry often proves to be a powerful tool. For the concerted cis addition of eq 1, two pathways are possible, leading to stereochemically different products. While both electronic and steric effects influence the direction of H_2 addition, these factors and their relative importance are difficult to analyze in a systematic way for complexes of the type *trans*-$IrX(CO)L_2$. In general, H_2 adds to *trans*-$IrX(CO)L_2$ according to pathway i with the phosphine ligands maintaining their trans disposition, but there are also reports of H_2 oxidative addition according to pathway ii. Bresadola et al. find that H_2 adds to complexes of the type *trans*-Ir(σ-carb)(CO)$(PPh_3)_2$ (carb = 1,2- and 1,7-dicarba-*closo*-dodecaborane(12)) via both pathways i and ii and that in moderately polar solvents isomerization then occurs favoring the isomer which would be formed by pathway i.[7] Steric crowding effects of the large carborane and phosphine ligands are invoked to explain the observed products. Harrod and co-workers report that H_2 adds to the reactive species $IrH(CO)(PPh_3)_2$ via both i and ii, giving a mixture of mer and fac isomers of $IrH_3(CO)(PPh_3)_2$,[8] and that group 4 hydrides, which are viewed as analogues of H_2, add to $IrH(CO)(PPh_3)_2$ according to pathway ii, as shown in eq 2.[9] A steric effect argument is put forth by these workers to account for the observed stereochemistry of the R_3SiH oxidative addition products,[10] but this argument is not applicable to the H_2 oxidative addition products.

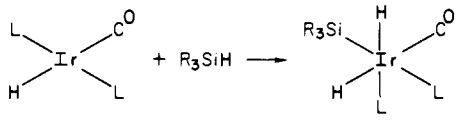

(2)

It is evident from these and other studies that much difficulty exists in evaluating the specific ligand effects which determine the stereochemistry of cis concerted additions to *trans*-$IrX(CO)L_2$, since in these systems the three ligands, X, CO, and L have widely varying steric *and* electronic properties. For cis phosphine analogues of $IrX(CO)L_2$, however, the influence of the phosphine ligand is essentially eliminated, and the electronic and steric effects of X and CO can be examined more analytically. In eq 3 the stereochemical consequences of the two pathways of concerted oxidative addition to *cis*-$IrX(CO)L_2$ are shown. For the product of each pathway, one hydride, and only one hydride, is trans to a phosphine ligand while the second hydride is cis to both phosphine ligands. Thus, in the cis complexes of $IrX(CO)L_2$ the phosphine ligands exert the same influence on the addend H_2 molecule regardless of pathway followed.

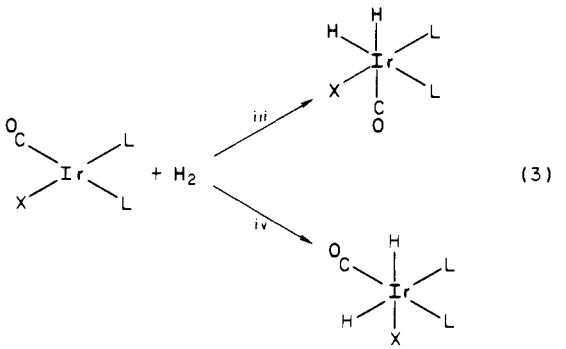

(3)

In this paper, we follow an approach based on this stereochemical analysis and describe studies probing the electronic and steric effects of X and CO ligands on the stereochemistry of H_2 oxidative addition to cis phosphine analogues of $IrX(CO)L_2$. Since different dihydride isomers will undoubtedly display different reactivities, control of the direction of H_2 addition may provide an important control on the rich reaction chemistry of these catalytically important dihydride species. Halpern, in fact, has suggested that differences in reactivity of the hydrogenation catalysts $Rh(PPh_3)_2^+$ and Rh(1,2-bis(diphenylphosphino)ethane)$^+$ may be the result of different stereochemistries of H_2 oxidative addition.[11] The complexes employed in our study are of the type IrX(CO)(dppe), where dppe is the cis chelating ligand $Ph_2PCH_2CH_2PPh_2$. The results of these studies are discussed in relation to current theories on the mechanism of H_2 oxidative addition. A preliminary report describing part of this work has appeared.[12]

Results and Discussion

Synthesis of Ir(I) dppe Compounds. The Ir(I) complexes of general formula **1** containing a single dppe chelate ring have been

(5) (a) Crabtree, R. H.; Hlatky, G. G. *Inorg. Chem.* **1980**, *19*, 571–2. (b) Crabtree, R. H. *Acc. Chem. Res.* **1979**, *12*, 331–8. (c) Crabtree, R. H.; Morehouse, S. M. *Inorg. Chem.* **1982**, *21*, 4210–3. (d) Crabtree, R. H.; Quirk, J. M. *J. Organomet. Chem.* **1980**, *199*, 99–106.

(6) (a) Blake has analyzed literature data for H_2 oxidative additions to $IrCl(CO)L_2$ and found a low correlation of ΔH with steric and electronic properties of the phosphine ligands. Mondal, J. U.; Blake, D. M. *Coord. Chem. Rev.* **1982**, *47*, 205–38. (b) Activation parameters may not be diagonistic of the oxidative addition mechanism for these complexes. Burgess, J.; Hacker, M. J.; Kemmitt, R. D. W. *J. Organomet. Chem.* **1974**, *72*, 121–6.

(7) Longato, B.; Morandini, F.; Bresadola, S. *Inorg. Chem.* **1976**, *15*, 650–6.

(8) Drouin, M.; Harrod, J. F. *Inorg. Chem.* **1983**, *22*, 999–1001.

(9) Fawcett, J. P.; Harrod, J. F. *J. Organomet. Chem.* **1976**, *113*, 245–8.

(10) Harrod, J. F.; Yorke, W. J. *Inorg. Chem.* **1981**, *20*, 1156–9.

(11) Halpern, J.; Riley, D. P.; Chan, A. S. C.; Pluth, J. J. *J. Am. Chem. Soc.* **1977**, *99*, 8055–7.

(12) Johnson, C. E.; Fisher, B. J.; Eisenberg, R. *J. Am. Chem. Soc.* **1983**, *105*, 7772–4.

synthesized and characterized. Compounds **1a–c** are prepared

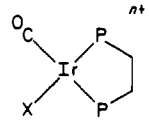

1a–d, X = Cl; Br, I, CN; $n = 0$
1e, X = PPh_3; $n = 1$

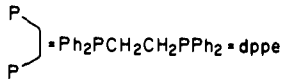

= $Ph_2PCH_2CH_2PPh_2$ = dppe

according to eq 4 as described previously,[12,13] and their IR and NMR data are collected in Table I. Yields of **1a–c** are limited

$$IrX_2(CO)_2^- + dppe \xrightarrow[-X^-]{THF} IrX(CO)_2(dppe) \xrightarrow{-CO} IrX(CO)(dppe) \quad (4)$$

by a secondary reaction with dppe, eq 5, forming the known bis(dppe) complex **3**.[14] Typical yields of **1a–c** from room-temperature reactions of $IrX_2(CO)_2^-$ and dppe are ca. 0%, 50%, and 75%, respectively. However, by performing the reaction at −80

$$IrX(CO)(dppe) + dppe \rightarrow Ir(CO)(dppe)_2^+X^- \quad (5)$$

°C under a CO atmosphere, **1a** can be obtained in 40% yield and the yield of **1b** improves to 75%. Under the reaction conditions employed here the mono(dppe) chelate complexes of Ir(I) exist mainly as the five-coordinate CO adducts **2a–c**, thus inhibiting the secondary reaction of **1a–c** with dppe, eq 5. Indeed, the order of CO affinity of **1a–c** parallels that of yield, **1c** > **1b** > **1a**. Qualitative estimates of CO affinity for **1a–c** were determined by applying a dynamic vacuum on THF solutions of **1a–c** which were initially stirred under an atmosphere of CO to generate **2a–c**. After 2 min of slow evacuation, IR spectra showed that **2a** was nearly completely converted to **1a**, **2b** was about 50% converted to **1b**, and **2c** remained essentially unchanged.

Previous attempts to synthesize mono(dppe) chelates of Ir(I) have been generally unsuccessful due to the prospensity for bis-chelate formation, as in eq 5. In 1966, Hieber and Frey reported the presumed synthesis of **2a** from $IrCl(CO)_2$(amine) and dppe,[14b] but Sanger has since shown by ^{31}P NMR spectroscopy that the actual product obtained was $[Ir(CO)(dppe)_2][IrCl_2(CO)_2]$.[15] Similarly, reports by Piraino, Faraone, et al. of **2a** prepared from $IrCl_2(CO)_2^-$ or $[IrCl(CO)_3]_n$ and dppe[16] are also in error. As above, the product must actually be a salt of $IrCl_2(CO)_2^-$ with $Ir(CO)(dppe)_2^+$ or $Ir(dppe)_2^+$. In fact, we find that the authentic complex **2a** cannot be isolated as a pure solid since in solution it readily loses CO forming the less soluble **1a**. Another potential route to the mono(dppe) complex **1a** is from the reaction of Vaska's complex, $IrCl(CO)(PPh_3)_2$, with dppe. Vaska's complex is known to readily exchange PPh_3 for other tertiary phosphine ligands, PR_3, forming $IrCl(CO)(PR_3)_2$.[14d,17] With dppe, however, the only product observed is the bis chelate **3**.[14a,c,d]

There appear to be only two prior reports of compounds of type **1** or **2**. Longato and Bresadola[18] have prepared an insoluble carborane complex, Ir(7-Ph-1,7-$B_{10}C_2H_{10}$)(CO)(dppe), from the reaction of Ir(7-Ph-1,7-$B_{10}C_2H_{10}$)(RCN)(CO)(PPh_3) (R = Me, Ph) with dppe, while Pilloni, Zotti, and Martelli[19] have prepared $Ir(SnPh_3)(CO)_2$(dppe) from the reaction of Ph_3SnCl with $Ir(CO)_2(dppe)^-$. The dicarbonyl anion was generated by electrochemical reduction of $Ir(dppe)_2^+$ under CO. Neither of these routes is applicable to the general synthesis of compounds of the type IrX(CO)(dppe), and therefore our efforts to synthesize other members of the series focused on halide substitution reactions with **1a–c**.

Cyanide complexes are prepared from **1b** or **1c** as summarized in eq 6. Complex **1d** is characterized by IR peaks for ν_{CO} (1997 cm^{-1}) and ν_{CN} (2118 cm^{-1}) and NMR data which closely match the spectra obtained for **1a–c** (Table I). The ^1H NMR spectrum

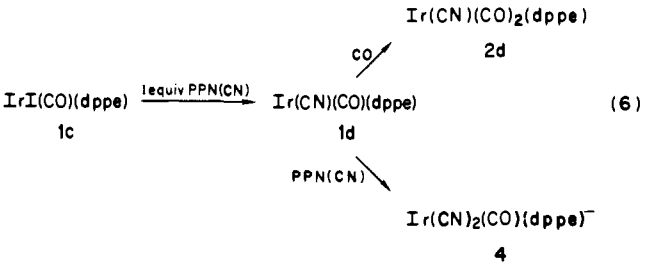

(6)

of **1d** exhibits four separate resonances for the dppe methylene H, while the $^{31}P\{^1H\}$ NMR spectrum consists of two doublets at 51.9 and 48.9 ppm with a P–P′ coupling of 13 Hz. The orange complex **1d** rapidly and reversibly reacts with CO to give colorless **2d** which can be precipitated from CO-saturated solutions. The IR spectrum of **2d** contains two peaks assignable to ν_{CO} at 2005 (m) and 1960 (s) cm^{-1} and one peak for ν_{CN} at 2140 (w) cm^{-1}. The ^1H NMR spectrum of **2d** exhibits single multiplets for methylene and *o*-phenyl protons which are characteristic of all of the five coordinate compounds **2** (see Table I). A singlet at δ 27.4 is observed in the $^{31}P\{^1H\}$ NMR spectrum. The observed chemical equivalence of dppe P and methylene H nuclei indicate that the five-coordinate compounds **2** are fluxional on the NMR time scale. It is likely that these 18-electron Ir(I) species adopt a trigonal-bipyramidal static structure such as C. IR spectra of **2a–d** contain two CO peaks of similar intensity indicative of a OC–Ir–CO bond angle close to 90°,[20] consistent with structure C.

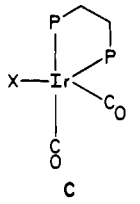

C

When 2 equiv of cyanide are added to **1b** or **1c**, the anionic complex $Ir(CN)_2(CO)(dppe)^-$ (**4**) forms, as characterized by a CO stretch at 1900 cm^{-1} and by NMR data indicative of five-coordinate complexes of the type $IrLL'_2$(dppe) which show single chemical shifts for dppe methylene and *o*-phenyl protons and for the phosphorus nuclei as shown in Table I.

Attempts to prepare cationic Ir(I) complexes containing a single dppe chelate also focused on halide substitution. The addition of 1 equiv of triphenylphosphine to **1b**, however, does not yield $Ir(CO)(PPh_3)(dppe)^+$ (**1e**) but instead gives a mixture of **3** and Vaska's bromide complex, $IrBr(CO)(PPh_3)_2$[21] (eq 7). When this reaction is followed by IR spectroscopy, evidence for two intermediates is observed. The IR spectrum 4 min after mixing

$$2IrBr(CO)(dppe) + 2PPh_3 \xrightarrow{acetone} [Ir(CO)(dppe)_2]Br + IrBr(CO)(PPh_3)_2 \quad (7)$$

contains three CO peaks: 1963 (s) cm^{-1} for $IrBr(CO)(PPh_3)_2$,

(13) Fisher, B. J.; Eisenberg, R. *Organometallics* **1982**, *2*, 764–7; *Inorg. Chem.* **1984**, *23*, 3216–22.
(14) (a) Vaska, L.; Catne, D. L. *J. Am. Chem. Soc.* **1966**, *88*, 5324–5. (b) Hieber, W.; Frey, V. *Chem. Ber.* **1966**, *99*, 2607–13. (c) Sacco, A.; Rossi, M.; Nobile, C. F. *J. Chem. Soc., Chem. Commun.* **1966**, 589–90. (d) Taylor, K. A. *Adv. Chem. Ser.* **1968**, *No. 70*, 195–206.
(15) Sanger, A. R. *J. Chem. Soc., Dalton Trans.* **1977**, 1971–6.
(16) Piraino, P.; Faraone, F.; Pietropaolo, R. *J. Chem. Soc., Dalton Trans.* **1972**, 2319–21; *Inorg. Nucl. Chem. Lett.* **1973**, *9*, 1237–41.
(17) Strohmeier, W.; Rehder-Stirnweiss, W.; Reischig, G. *J. Organomet. Chem.* **1971**, 393–7.
(18) Longato, B.; Bresadola, S. *Inorg. Chim. Acta* **1979**, *33*, 189–93.
(19) Pilloni, G.; Zotti, G.; Martelli, M. *Inorg. Chim. Acta* **1975**, *13*, 213–8.
(20) (a) Kettle, S. F. A.; Paul, I. *Adv. Organomet. Chem.* **1972**, *10*, 199–236. (b) Beck, W.; Melnikoff, A.; Stahl, R. *Angew. Chem., Int. Ed. Engl.* **1965**, *4*, 692–3; *Chem. Ber.* **1966**, *99*, 3721–7.
(21) (a) Vaska, L.; DiLuzio, J. W. *J. Am. Chem. Soc.* **1961**, *83*, 2784–5. (b) Angoletta, M. *Gazz. Chim. Ital.* **1959**, *89*, 2359–70.

Table II. IR, ^1H NMR, and ^{31}P NMR Data of Hydride Complexes[a]

compound	ν_{CO}, cm^{-1}	ν_{IrH}, cm^{-1}	δ_{CH_2}	$\delta_{o\text{-}C_6H_5}$[b]	δ_{IrH} (phosphorus couplings)	$J_{HIrH'}$	$^{31}P\{^1H\}$ NMR
$IrH_2Cl(CO)(dppe)$ (**5a**)			3.19 (1 H), 2.80 (2 H), 2.46 (1 H)	8.05 (4 H), 7.92 (2 H), 7.67 (2 H)	−8.10 (14.6, 150.9), −8.76 (18.4, 20.8)	*e*	34.2, 15.1[f]
$IrH_2Br(CO)(dppe)$[g] (**5b**)	2000[c]	2105[c]	3.19, 2.82, 2.75, 2.47	8.04, 7.99, 7.93, 7.69	−8.70 (13.1, 148), −9.49 (−19.1[d])	*e*	36.7, 14.2[f]
$IrH_2I(CO)(dppe)$ (**5c**)			3.18 (1 H), 2.78 (2 H), 2.49 (1 H)	7.97 (4 H), 7.89 (2 H), 7.71 (2 H)	−9.85 (12.1, 143.9), −10.82 (−18.4[d])	1.5	34.7, 12.1[f]
$IrH_2(CN)(CO)(dppe)$[h] (**5d**)	2005	2105	3.25 (1 H), 2.88 (2 H), 2.50 (1 H)	7.97 (4 H), 7.88 (2 H), 7.67 (2 H)	−10.13 (13.2, 129.9), −10.87 (−17.9[d])	*e*	31.2, 18.3[f]
$[IrH_2(PPh_3)(CO)(dppe)]NO_3$ (**5e**)	2020		3.13 (2 H), 2.73 (2 H)	8.07 (2 H), 7.80 (2 H)[i]	−10.06 (10.5, 19, 115), −10.24 (−17[j])	2.4	33.7, 24.6, 6.9[n]
$IrH_3(CO)(dppe)$[k] (**5g**)	1960	2075, 2020	2.84 (2 H), 2.56 (2 H)	7.88 (4 H), 7.71 (4 H)	−10.54 (−11.5, 125.9), −11.61 (19.6)	*e*	30.8 (s)[m]
$IrH_2Cl(CO)(dppe)$ (**6a**)	2045	2205	3.07 (2 H), 2.65 (2 H)	7.87 (2 H), 7.76 (4 H), 7.65 (2 H)	−8.68 (17.2, 131.4), −19.01 (8.8, 17.2)	5.2	
$IrH_2Br(CO)(dppe)$ (**6b**)	2040	2200	3.13 (2 H), 2.62 (2 H)	7.79 (4 H), 7.68 (4 H)	−9.08 (16.5, 129.7), −18.08 (9.3, 17.0)	5.5	35.4, 28.1[f]
$IrH_2I(CO)(dppe)$[l] (**6c**)	2035	2175	3.18 (2 H), 2.77 (1 H), 2.55 (1 H)	7.82, 7.77, 7.70, 7.62	−9.91 (16.9, 127.3), −16.22 (8.9, 17.0)	4.7	30.6, 23.1[f]
$IrH_2(CN)(CO)(dppe)$ (**6d**)					−10.43 (16.1, 121), −13.27 (12.5, 19.3)	4.9	31.9, 24.8[f]
$IrH_2(CN)(CO)(dppe)$ (**7d**)					−9.88 (−10.4, 131.6)		
$PPN[IrH_2(CN)_2(dppe)]$ (**8**)			2.74 (1 H), 2.48 (2 H), 2.26 (1 H)	8.13 (2 H), 8.06 (2 H), 7.90 (4 H)	−10.47 (16.3, 147), −14.52 (14.0, 17.9)	4.0	35.1, 18.7[f]

[a] See footnote *a*, Table I. [b] See footnote *b*, Table I. [c] THF solution. [d] Unresolved doublet of doublets. [e] Coupling not resolved. [f] P–P coupling not resolved. Selective ^1H decoupling shows that the upfield resonance is coupled to a trans hydride. [g] For **5b**-d_2, ν_{CO} = 2050 cm^{-1} in THF. [h] ν_{CN} = 2132 cm^{-1}. For **5d**-d_2, ν_{CO} = 2050 cm^{-1} and ν_{CN} = 2133 cm^{-1}. [i] The rest of the phenyl resonances of dppe and PPh_3 are in the region δ 7.25–7.65. [j] An approximate quartet due to three nearly equivalent phosphorus couplings. [k] The ^1H NMR spectrum has been simulated in ref 13, and the coupling between equivalent hydrides is 4.5 Hz. For **5g**-d_3, ν_{CO} = 2030 cm^{-1} (ref 13). The IR spectrum of **5g** is reassigned here. [l] For **6c**-d_2, ν_{CO} = 2037 cm^{-1}. [m] Benzene solution. [n] The peak at δ 6.9 (dd, $J_{PP'}$ = 13, 163 Hz) is assigned to PPh_3 and is coupled to each P of dppe, δ 33.7 (d, $J_{PP'}$ = 163 Hz, dppe P trans to PPh_3) and δ 24.6 (d, $J_{PP'}$ = 13 Hz, dppe P trans to H as confirmed by selective decoupling).

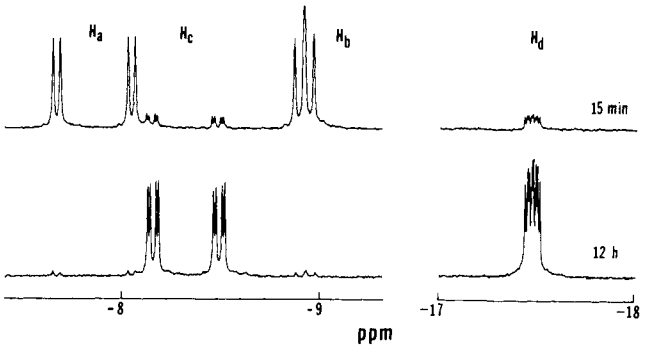

Figure 1. ^1H NMR spectra (400 MHz) in the hydride region for the reaction of IrBr(CO)(dppe) (**1b**) with H_2 in benzene solution. The resonances are assigned to the hydrides of **5b** and **6b** according to eq 9 in the text.

1915 (s) cm^{-1}, and 2008 (w) cm^{-1}. The latter two peaks disappear over the course of 20 min and a new peak grows in at 1940 cm^{-1} for **3**. An orange-yellow crystalline precipitate then forms, which when collected and isolated is identified as $IrBr(CO)(PPh_3)_2$ by its IR spectrum and its reaction with H_2 to give $IrH_2Br(CO)(PPh_3)_2$ (determined by ^1H NMR spectroscopy[22] in comparison with an authentic sample). The IR peaks at 1915 and 2008 cm^{-1} are in the regions expected for $IrBr(PPh_3)(CO)(dppe)$ and $Ir(PPh_3)(CO)(dppe)^+$ (**1e**), two likely intermediates for this reaction. Given the results of eq 7, it is clear why the reaction of $IrCl(CO)(PPh_3)_2$ with dppe does not yield **1a**. Quite simply, **1a** is not stable in the presence of PPh_3. The ease of substitution of the chelate dppe by PPh_3 is somewhat surprising, but apparently the driving force for the reaction comes from the formation of **3**.

The in situ preparation of the desired triphenylphosphine dppe complex **2e** is achieved by first removing the halide ligand as its silver salt and then adding PPh_3, eq 8. The reaction probably proceeds via a cationic intermediate such as **2f** in eq 8. The complex **2e** is identified by the IR and NMR data given in Table I.

$$\underset{\textbf{1b}}{IrBr(CO)(dppe)} \xrightarrow[AgNO_3]{CO} \underset{\textbf{2f}}{Ir(CO)_3(dppe)^+} \xrightarrow{PPh_3} \underset{\textbf{2e}}{Ir(PPh_3)(CO)_2(dppe)^+} \quad (8)$$

Reaction of H_2 with IrX(CO)(dppe) (X = Cl, Br, I). The halide complexes **1a–c** react with H_2 in solution to form sequentially two isomeric dihydride species **5** and **6**, eq 9. The reaction has been followed by IR and ^1H and ^{31}P NMR spectroscopies which allow for the unequivocal assignment of each isomer (see Table II).

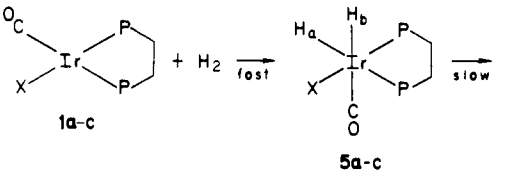

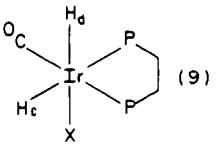

(9)

Figure 1 shows the hydride region of ^1H NMR spectra of a benzene solution of **1b** under H_2 taken 15 min and 12 h after mixing. Samples in this study were typically prepared on a high-vacuum line by condensing 0.5 mL of C_6D_6 into an NMR tube containing 6 mg of complex and then flame sealing the tube under H_2. The initial spectrum of Figure 1 contains two major hydride peaks, a doublet of doublets at δ −7.87 containing cis and trans phosphorus couplings (14.2 and 152.2 Hz, respectively) assigned to H_a of **5b**, and an approximate triplet at δ −8.94 containing two nearly equivalent cis phosphorus couplings (~19.3 Hz) assigned to H_b of **5b**. Over the course of several hours, these peaks diminish as a second set of hydride multiplets grow in. the

(22) Ginsberg, A. P. *Transition Metal Chem.* **1965**, *1*, 172.

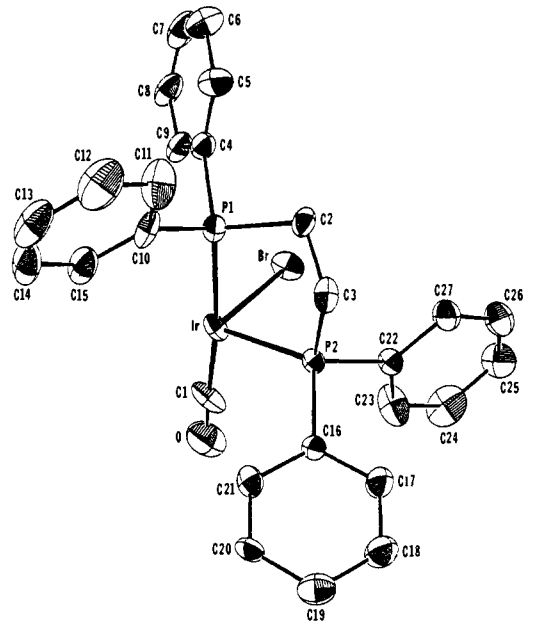

Figure 2. Perspective ORTEP drawing of $IrH_2Br(CO)(dppe)$ (**6b**) with 30% probability thermal ellipsoids. The hydride ligands were not located in the structure determination and are not shown.

secondary product has a doublet of doublets of doublets at δ −8.34 assigned to H_c of **6b** containing cis and trans phosphorus couplings (17.2 and 139.2 Hz, respectively) and H–H coupling (5.2 Hz) and another ddd at δ −17.48 containing two cis phosphorus couplings and H–H coupling (8.6, 16.6, and 5.2 Hz, respectively) assigned to H_d of **6b**. The upfield chemical shift position of H_d in **6a–c** is characteristic of a hydride trans to halide.[23] IR spectra further substantiate these assignments. Compound **5b** exhibits a CO stretch at 2000 cm^{-1} and an Ir–H stretch at 2105 cm^{-1}. The corresponding dideuteride, **5b**-d_2, prepared from **1b** and D_2, has a single peak at 2050 cm^{-1}; this shift of ν_{CO} to higher energy upon deuteration is diagnostic for a CO ligand trans to hydride.[24] IR spectra of **6a–c** contain a CO stretch at 2035–2045 cm^{-1} which is unaffected by deuteration and an Ir–H stretch at 2175–2205 cm^{-1}. The Ir–H stretch is in the high energy region expected for a hydride trans to halide.[23,24]

The above structural assignments for **5a–c** and **6a–c** are confirmed by an X-ray crystal structure of complex **6b**. The molecular structure of **6b** is shown in Figure 2, Table III contains the non-hydrogen atomic coordinates along with isotropic equivalent thermal parameters, and Table IV lists selected bond distances and angles. Although the hydride ligands could not be unambigously located in the structure determination, the compound clearly has the predicted configuration in which the CO ligand is trans to one phosphorus donor (P1–Ir–C angle, 174.1°) while Br is cis to both phosphorus donors and trans to a coordination site presumably occupied by a hydride ligand. The iridium bromine distance, 2.596 (1) Å, is toward the higher end of the range found in similar complexes (2.515–2.638 Å)[25] and is close to that observed in two other compounds where the trans ligand is hydride (2.612 and 2.625 Å).[25b,d] The relatively long Ir–Br bond

Table III. Positional Parameters and Their Estimated Standard Deviations

atom	x	y	z	B(iso equiv)[a]
Ir	0.91618 (3)	0.87803 (3)	0.99094 (3)	3.319 (7)
Br	1.09133 (8)	0.96167 (6)	0.9900 (1)	4.72 (2)
P1	0.8156 (2)	0.9821 (2)	1.0549 (2)	3.16 (6)
P2	0.9378 (2)	0.8471 (2)	1.1768 (2)	2.66 (5)
O	1.032 (1)	0.7473 (6)	0.8939 (9)	8.7 (3)
C1	0.989 (1)	0.7973 (7)	0.926 (1)	5.6 (3)
C2	0.8514 (9)	0.9923 (7)	1.2003 (8)	3.7 (2)
C3	0.8516 (9)	0.9152 (7)	1.2544 (8)	3.6 (3)
C4	0.8385 (7)	1.0771 (5)	0.997 (1)	3.8 (2)
C5	0.798 (1)	1.1422 (7)	1.046 (1)	5.6 (3)
C6	0.814 (1)	1.2131 (7)	0.998 (1)	7.4 (4)
C7	0.870 (1)	1.2186 (8)	0.901 (1)	6.6 (3)
C8	0.907 (1)	1.1557 (7)	0.849 (1)	5.3 (3)
C9	0.8944 (9)	1.0844 (7)	0.8957 (9)	4.3 (3)
C10	0.6681 (8)	0.9679 (7)	1.0507 (9)	4.1 (3)
C11	0.600 (1)	1.007 (1)	1.128 (1)	6.7 (4)
C12	0.490 (1)	0.995 (1)	1.121 (1)	8.2 (5)
C13	0.4436 (9)	0.9526 (8)	1.044 (1)	6.8 (4)
C14	0.5071 (9)	0.9184 (7)	0.970 (1)	7.0 (3)
C15	0.6204 (9)	0.9251 (7)	0.971 (1)	5.6 (3)
C16	0.8926 (8)	0.7536 (6)	1.2258 (8)	2.8 (2)
C17	0.9362 (9)	0.7234 (7)	1.3210 (9)	4.5 (3)
C18	0.898 (1)	0.6540 (7)	1.360 (1)	5.4 (3)
C19	0.819 (1)	0.6123 (7)	1.307 (1)	5.0 (3)
C20	0.7739 (9)	0.6451 (6)	1.2125 (9)	3.6 (2)
C21	0.8113 (8)	0.7131 (7)	1.1720 (9)	3.6 (2)
C22	1.0742 (9)	0.8546 (6)	1.2291 (8)	3.2 (2)
C23	1.154 (1)	0.8063 (9)	1.188 (1)	6.4 (4)
C24	1.259 (1)	0.811 (1)	1.224 (1)	7.7 (5)
C25	1.2862 (9)	0.8690 (9)	1.301 (1)	6.1 (4)
C26	1.213 (1)	0.9142 (8)	1.339 (1)	6.9 (4)
C27	1.102 (1)	0.9110 (8)	1.309 (1)	5.7 (3)

[a] The isotropic equivalent thermal parameter is defined as (4/3)-[$aaB(1,1) + bbB(2,2) + ccB(3,3) + ab(\cos\gamma)B(1,2) + ac(\cos\beta)B(1,3) + bc(\cos\alpha)B(2,3)$].

Table IV. Selected Bond Distances and Angles in $IrH_2Br(CO)(dppe)$ (**6b**)

	Distances, Å		
Ir–Br	2.596 (1)	P1–C4	1.817 (9)
Ir–P1	2.324 (3)	P1–C10	1.830 (10)
Ir–P2	2.344 (2)	P2–C3	1.847 (10)
Ir–C1	1.839 (13)	P2–C16	1.815 (9)
C1–O	1.088 (14)	P2–C22	1.798 (10)
P1–C2	1.834 (9)	C2–C3	1.491 (15)
	Angles, deg		
Br–Ir–P1	90.46 (7)	Ir–P2–C16	119.2 (3)
Br–Ir–P2	92.21 (6)	Ir–P2–C22	115.6 (3)
Br–Ir–C1	91.1 (4)	C2–P1–C4	104.8 (5)
P1–Ir–P2	85.06 (9)	C2–P1–C10	106.1 (5)
P1–Ir–C1	174.1 (4)	C4–P1–C10	105.4 (4)
P2–Ir–C1	100.6 (5)	C3–P2–C16	103.2 (4)
Ir–C1–O	176 (1)	C3–P2–C22	107.8 (4)
Ir–P1–C2	105.7 (3)	C16–P2–C22	103.5 (4)
Ir–P1–C4	119.4 (4)	P1–C2–C3	110.0 (7)
Ir–P1–C10	114.3 (4)	P2–C3–C2	110.4 (6)
Ir–P2–C3	106.5 (3)		
	Torsional Angle, deg		
	P1–C2–C3–P2	52.4	

is consistent with the known high trans influence of the hydride ligand.[24b,26]

For all halides, the conversion of orange IrX(CO)(dppe) (**1**) to colorless $IrH_2X(CO)(dppe)$ is complete in less than 1 min in solution under an atmosphere of H_2 at 25 °C, and ^1H NMR spectra show that isomer **5** of the dihydride forms with >99% stereoselectivity. Under vacuum the orange color of **1** returns within a couple minutes, indicating ready reversibility of H_2 oxidative addition. The subsequent isomerization of **5** to **6** proceeds over the course of several hours at 25 °C in benzene, eventually

(23) (a) Kaesz, H. D.; Saillant, R. B. *Chem. Rev.* **1972**, *72*, 231–81. (b) Jesson, J. P. In "Transition Metal Hydrides"; Muetterties, E. L., Ed.; Marcel Dekker: New York, 1971; Chapter 4. (c) Olgemoller, B.; Beck, W. *Inorg. Chem.* **1983**, *22*, 997–8. (d) Chatt, J.; Johnson, N. P.; Shaw, B. L. *J. Chem. Soc.* **1964**, 1625–31. (e) Chatt, J.; Coffey, R. S.; Shaw, B. L. *Ibid.* **1965**, 7391–405. (f) Birnbaum, E. R. *Inorg. Nucle. Chem. Lett.* **1971**, *7*, 233–7.

(24) (a) Vaska, L. *J. Am. Chem. Soc.* **1966**, *88*, 4100–1. (b) Appleton, T. G.; Clark, H. C.; Manzer, L. E. *Coord. Chem. Rev.* **1973**, *10*, 335–422.

(25) (a) Thorn, D. L.; Tulip, T. H. *J. Am. Chem. Soc.* **1981**, *103*, 5984–6. (b) Von Deuten, K.; Dahlenburg, L. *Cryst. Struct. Commun.* **1980**, *9*, 421. (c) Churchill, M. R.; Julis, S. A. *Inorg. Chem.* **1979**, *18*, 1215–21. (d) Behrens, U.; Dahlenburg, L. *J. Organomet. Chem.* **1976**, *116*, 103–11. (e) Brotherton, P. D.; Raston, C. L.; White, A. H.; Wild, S. B. *J. Chem. Soc., Dalton Trans.* **1976**, 1799–802. (f) Churchill, M. R.; Hackbarth, J. J. *Inorg. Chem.* **1975**, *14*, 2047–51.

(26) Robertson, G. B.; Tucker, P. A. *J. Am. Chem. Soc.* **1982**, *104*, 317–8.

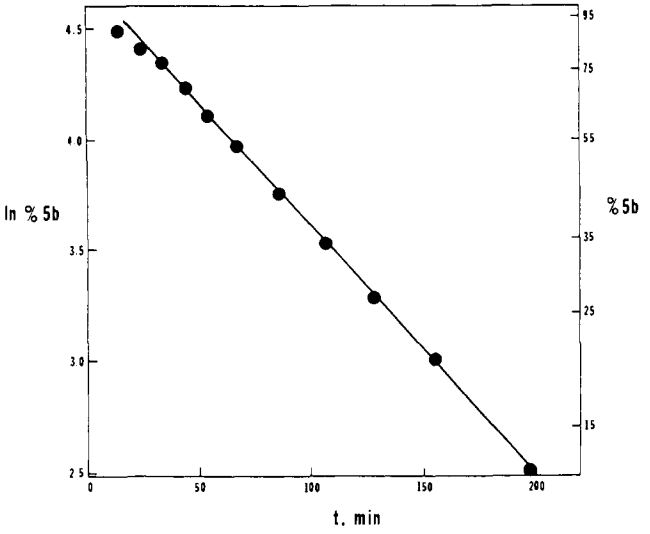

Figure 3. Plot of ln [**5b**] vs. time for the isomerization of **5b** to **6b** where the concentration of **5b** is expressed in percent such that % **5b** + % **6b** = 100%. The total iridium complex concentration is 1.9×10^{-2} M.

reaching an equilibrium (K = 41, 35, 13 for X = Cl, Br, I, respectively). While **6** can in principle form by direct oxidative addition of H_2 to the Ir(I) complexes **1** along pathway iv in eq 3, the observation of >99% stereoselective formation of **5** indicates that the H_2 oxidative addition reaction is proceeding under kinetic control, with the approach of H_2 to **1** via pathway iii in eq 3 favored over that of pathway iv by >2.7 kcal/mol.

Isomerization Mechanism for the Interconversion of 5a–c and 6a–c. The isomerization of $IrH_2X(CO)(dppe)$ from **5** to **6** has been studied kinetically in both benzene and acetone solvents. The progress of the reaction was followed by ^1H NMR integration of the hydride resonances for **5** and **6**. Since exposure to fluorescent roomlight was observed to accelerate the reaction, all samples were maintained in darkness until transfer to the NMR probe.

The isomerization reaction exhibits distinctly different behavior in benzene and acetone solutions. In benzene the reaction is typically half-complete in 2 h at 25 °C, but consistently reproducible kinetics have not been obtained. The isomerization rate depends slightly on the halide with times for 50% isomerization of 60, 80, and 100 min at 35 °C for Cl, Br, and I, respectively. When 4 equiv of tetrabutylammonium (TBA) bromide are added to the reaction solution, the isomerization of **5b** proceeds more slowly, with a half-life of about 30 h at 25 °C. Contacting a benzene solution of **5c** with solid $AgBF_4$ for 10 min greatly accelerates the isomerization rate with **5c** 86% isomerized to **6c** in 20 min. In this reaction, only compounds **5c** and **6c** are observed by ^1H NMR, indicating that only a trace of Ir complex reacts with the insoluble $AgBF_4$ or that other products are insoluble in benzene. As a test for monohydride intermediates, the isomerization reaction was studied by using a mixture of H_2 and D_2. Compound **1c** was reacted with a 47:53 mixture of H_2 and D_2 to give **5c** and **5c**-d_2. After removing excess H_2 and D_2 with two freeze–pump–thaw cycles, the isomerization reaction was followed by ^1H NMR spectroscopy. The spectra show that the isomerization proceeds largely without H/D scrambling. After 5 h the sample was 62% isomerized to **6c** with only 3% scrambling to **6c**-d_1. A fortuitous isotope shift in the upfield hydride resonance (9 Hz separation in the 400 MHz spectrum) resulted in nearly base line separation of the overlapping resonances for **6c**-d_0 and **6c**-d_1, thus allowing for accurate analysis of the isotopic composition. Eventually, H/D randomization does occur, and after 42 h there was 39% scrambling in **6c** to the **6c**-d_1 isotopomers.

In acetone solution the isomerization half-life for **5b** is about 35 h at 25 °C. At 55 °C the reaction proceeds with good first-order kinetics as shown by the linear plot of ln [**5b**] vs. time in Figure 3. The observed first-order rate constant is 0.011 min^{-1} which corresponds to a half-life of 62 min. In the presence of 2.5 equiv of [TBA]Br the reaction proceeds only slightly slower with a half-life of 90 min. To check for the possibility of acid–base chemistry[27] in the isomerization of **5b** to **6b**, the reaction was carried out under a hydrogen atmosphere in the presence of 100 equiv of D_2O. Very little incorporation of the deuterium label occurred during the isomerization. After 42 h there was less than 10% deuterium incorporation into **6b** (the sample was 63% isomerized to **6b** at this time).

The differing results in acetone and benzene solvents clearly cannot be explained by a single reaction mechanism. In acetone solution, where the isomerization follows clean first-order kinetics, we consider two possible mechanisms. The first is a simple intramolecular rearrangement and the second is a two-step H_2 reductive elimination/oxidative addition process shown in eq 10. While both mechanisms satisfy the observed first-order kinetics for **5**, the mechanism in eq 10 requires that the rate of reductive

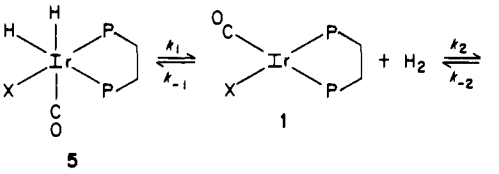

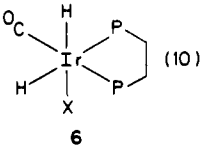

(10)

elimination of H_2 from **5** is much fasfer than the rate of isomerization, since **1** preferentially adds H_2 to give **5** with >99% stereoselectivity. Kinetically, this observed stereoselectivity requires that $k_{-1}/k_2 > 100$. If the rate-determining step in the isomerization shown in eq 10 is assumed to involve k_2, and a steady state approximation is followed ignoring k_{-2}, then one obtains the rate equation for the isomerization given as (11). Incorporation of

$$\text{rate} = k_{obsd}[5] = \frac{k_1 k_2}{k_{-1} + k_2}[5] = \frac{k_1}{k_{-1}/k_2 + 1}[5] \quad (11)$$

the observed stereoselectivity of H_2 oxidative addition (i.e., $k_{-1}/k_2 > 100$) into eq 11 reveals the requirement that $k_1 > 100k_{obsd}$ where k_{obsd} is the observed rate of isomerization. Equation 11, which predicts first-order kinetics in **5**, would accurately fit the data until the reaction approaches equilibrium and k_{-2} becomes important (at about 80% conversion).

In order to test the validity of the mechanism given in eq 10 and its associated rate law, we have determined k_1 directly by following the reaction of **5b** with D_2 by ^1H NMR spectroscopy. In both benzene and acetone solvent **5b** is converted to **5b**-d_2 prior to isomerization to **6b** with a half-life of 10 min at 25 °C. Integration of the hydride resonances of **5b** against those of the corresponding dppe methylene or phenyl hydrogens gives the relative amounts of **5b** and **5b**-d_2. Similar results are obtained by following the reaction of **5b** with CO which gives **2b**, presumably also via reductive elimination of H_2 from **5b**. Since the isomerization half-life is 35 h in acetone solution, the ratio k_1/k_{obsd} is ~200. Thus, the requirement that $k_1 > 100k_{obsd}$ is satisfied and the mechanism in eq 10 is consistent with all of the kinetic data. If this mechanism is correct, then the actual H_2 oxidative addition stereoselectivity is 99.5%.

Precedent for the isomerization for an Ir hydride complex via reductive elimination/oxidative addition has been established by Harrod et al.[10] in the interconversion of mer and fac isomers of $IrH_3(CO)(PPh_3)_2$, eq 12. The most compelling evidence in favor of this mechanism over that of an intramolecular rearrangement reaction is the observation that the isomerization rate is nearly the same as the rate of PPh_3 substitution into $IrH_3(CO)(PPh_3)_2$ forming $IrH(CO)(PPh_3)_3$. Both reactions appear to proceed via rate-determining reductive elimination of H_2. Intramolecular

(27) Anton, D. R.; Crabtree, R. H. *Organometallics* **1983**, *2*, 621–7.

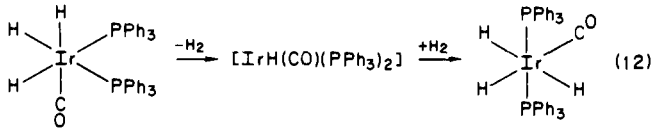

(12)

isomerization that does not involve reductive elimination/oxidative addition has been demonstrated for Ir hydrides of the type cis-trans-$IrH_2(dppe)_2^+$[28] and $IrHCl(dppe)_2^+$,[29] and it has also been suggested for H/D scrambling in a mono-chelate complex, eq 13.[30]

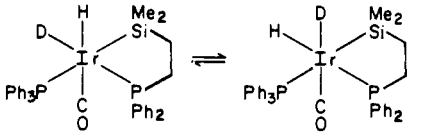
(13)

The latter reaction is proposed to proceed via intramolecular rearrangement although the possibility of an intramolecular pathway involving Si–H(D) reductive elimination/oxidative addition has not been ruled out.[31] While the results elucidating the isomerization mechanism of **5** and **6** in acetone are not unambiguous, the isomerization most likely involves H_2 reductive elimination and oxidative addition given the result that the rate of H_2 reductive elimination is much faster than the rate of isomerization.

In benzene solution the isomerization rate is about ten times faster than in acetone, and neither of the above first-order mechanisms is consistent with the results. In particular, neither mechanism accounts for the 15-fold rate inhibition of added [TBA]Br or the rate acceleration by $AgBF_4$. These results could possibly be explained by a mechanism involving reversible loss of Br^- from **5b**. Accordingly, we have attempted to measure the rate of Br^- loss from **5b** by examining the reaction of **5b** with CN^-, eq 14. Since PPN(CN) is not sufficiently soluble in benzene, acetone was used as the solvent. A solution of **5b** under 600 torr

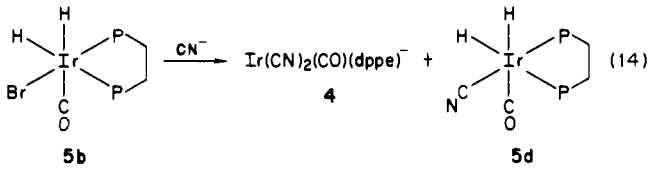

(14)

of H_2 was mixed with 3 equiv of PPN(CN) and the sample flame-sealed. Complexes **4** and **5d** were identified as the principal products formed in a 30:1 ratio. The characterization of **5d** (Table II) will be discussed in the section dealing with the chemistry of **1d** and H_2. The starting complex **5b** reacts with a half-life of about 10 min which is the same as the known rate of H_2 reductive elimination. Thus, **4** undoubtedly forms via the previously established reaction of H_2 reductive elimination from **5b** forming **1b**, which then reacts with 2 equiv of CN^-.

The minor product of eq 14, **5d**, may result from CN^- coordination after Br^- dissociation from the kinetic isomer **5b**, but it could also form via H_2 addition to Ir(CN)(CO)(dppe) (**1d**), a presumed intermediate in the formation of **4**. If Br^- dissociation from **5b** does occur in acetone solution, it must proceed at least 30 times slower than H_2 reductive elimination from **5b** based on the observed product ratio of eq 14 and therefore have a half-life of ≥5 h. In the nonpolar benzene solvent, Br^- dissociation should occur even less readily. Since the observed half-life for isomerization in benzene is 2 h, an isomerization mechanism involving reversible Br^- loss appears incompatible.

The isomerization of **5** and **6** in benzene solution has also been studied in the reverse direction, **6** → **5**. Since the equilibrium amount of **5** is only a few percent, the reaction is most easily studied by trapping isomer **5** as it forms. At equilibrium the forward and reverse rates of isomerization will be equal and the reverse-isomerization rate constant can be calculated as $k_r = k_f/K_{eq}$. In acetone solution where the half-life for isomerization is about 35 h at room temperature, the half-life for reverse isomerization should be ~50 days. In benzene solution the estimated half-life for reverse isomerization is about 2 days. Three different traps for isomer **5** have been used: D_2, CO, and PPh_3. The reactions are followed by ^1H NMR spectroscopy and proceed nearly completely to a single product in each case. For the case of D_2, the reverse isomerization rate should be equal to the rate of disappearance of **6**-d_0, assuming that deuteration occurs only after isomerization to **5**. ^1H NMR spectra of a solution of **6c** under 600 torr of D_2 show the formation of the equilibrium amount of **5c**-d_2 (7%) over the course of several hours, while the disappearance of **6c**-d_0 and appearance of **6c**-d_2 proceed with a half-life of about 48 h. Similar results are obtained under a CO atmosphere, in which case **6c** is converted to $IrI(CO)_2(dppe)$ (**2c**) with a room-temperature half-life of about 30 h. The magnitude and qualitative agreement in rates for the CO and D_2 reactions are consistent with a common rate-determining step corresponding to the reverse isomerization process, **6** → **5**.

However, when PPh_3 is used to trap isomer **5b** from the isomerization of **6b**, different and possibly conflicting results are obtained. A benzene solution of **6b** containing 15 equiv of PPh_3 was sealed in an NMR tube under 600 torr of D_2 and monitored by ^1H NMR spectroscopy. A single product, $IrD_2(PPh_3)(CO)(dppe)^+$ (**5e**-d_2), is observed to form very slowly with a room-temperature half-life for reaction of ~90 days, eq 15. The product **5e** is identified by its characteristic dppe methylene and *o*-phenyl resonances (Table II). No D_2 exchange with **6b** occurs during this time, in contrast to the previously described reaction of **6c** with D_2 in the absence of PPh_3. Complex **5e** has been inde-

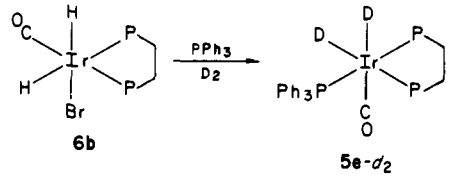

(15)

pendently prepared from IrBr(CO)(dppe) (**1b**) + H_2 + PPh_3 and from $Ir(PPh_3)(CO)_2(dppe)^+$ (**2e**) + H_2 as described in a following section. On the basis of these independent syntheses we conclude that **5e** forms in eq 15 because either **1b** or **5b** (which readily eliminates H_2) is generated as an intermediate. The rate of reaction 15 is about 40 times slower than the reverse isomerization rate measured under D_2 and CO, but it agrees with the calculated rate for reverse isomerization in acetone solution, i.e., ~50 day half-life. Thus there appear to be two different isomerization mechanisms in benzene—a slow mechanism which may well be the same as that operating in acetone solution and probably involves H_2 reductive elimination/oxidative addition, and a fast mechanism which remains to be elucidated. The fast isomerization mechanism in benzene solution may involve catalysis by trace impurities or radicals, and these possibilities are being investigated.

Reaction of H_2 with Ir(CN)(CO)(dppe). Solutions of Ir(CN)(CO)(dppe) (**1d**) or its CO adduct, **2d**, rapidly react with H_2 at 25 °C to form exclusively dihydride **5d**, eq 16. Complex

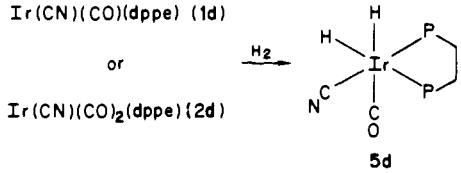

(16)

5d is characterized spectroscopically by the data in Table II which

(28) Brown, J. M.; Dayrit, F. M.; Lightowler, D. *J. Chem. Soc., Chem. Commun.* **1983**, 414–5.
(29) Miller, J. S.; Caulton, K. G. *J. Am. Chem. Soc.* **1975**, *97*, 1067–73.
(30) Auburn, M. J.; Stobart, S. R. *J. Chem. Soc., Chem. Commun.* **1984**, 281–2.
(31) Although this pathway would require four steps involving oxidative addition or reductive elimination of Si–H(D) (i.e., initial SiD reductive elimination followed by SiD oxidative addition along the H–Ir–CO axis, then SiH reductive elimination followed by SiH oxidative addition along the P–Ir–P axis), the analgous chemistry with H_2 is known (see ref 10).

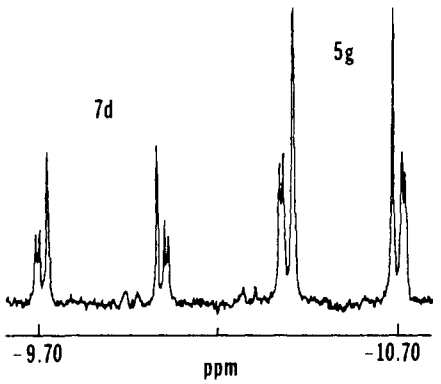

Figure 4. ^1H NMR spectrum (400 MHz) showing the AA'XX' hydride resonances of isomer **7d** of $IrH_2(CN)(CO)(dppe)$ and $IrH_3(CO)(dppe)$ (**5g**). Complex **5g** has a second hydride resonance at δ −11.61 which is not shown in the figure.

compare favorably with that for the corresponding halide complexes **5a–c**. The ^1H NMR spectrum contains peaks for dppe protons and two hydrides, one of which is trans to phosphorus (δ −10.13 with trans J_{PH} = 129.9 Hz). The IR spectrum of **5d** has bands at 2132 (m), 2105 (m), and 2005 (ms) cm^{-1}, corresponding respectively to ν_{CN}, ν_{IrH}, and ν_{CO} trans to hydride, while the dideuteride complex **5d**-d_2, prepared from **1d** and D_2, has bands at 2133 (m) and 2050 (s) cm^{-1} for ν_{CN} and ν_{CO} trans to deuteride.

Upon heating or standing for several days at 25 °C **5d** equilibrates with two other isomers, **6d** and **7d**, eq 17. After heating

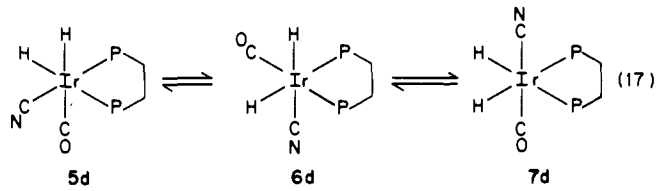

an acetone solution of **5d** at 90 °C for 25 min and then cooling quickly to room temperature, the solution contains 82% **5d**, 11% **6d**, and 7% **7d**. At room temperature the composition shifts over several days to an apparent equilibrium of 89% **5d**, 5% **6d**, and 6% **7d**. Subsequent heating regenerates the high-temperature composition, indicating that the three species are indeed in equilibrium. Complex **6d** is characterized by ^1H and ^{31}P NMR data in Table II closely parallelling that for the corresponding halide complexes, **6a–c**. As expected, the chemical shift of the hydride trans to CN in **6d**, δ −13.27, is intermediate between the ranges observed for H trans to CO or P (δ −8 to −11) and H trans to halide (δ −16 to −19). Complex **7d** is characterized primarily by the distinctive pattern of its ^1H NMR hydride resonance which is indicative of two hydrides trans to equivalent phosphine ligands. Figure 4 shows the hydride resonance of **7d** which results from an AA'XX' spin system where the A–X and A–X' couplings differ by an order of magnitude and are opposite in sign. A very similar pattern is observed for *fac*-$IrH_3(CO)(dppe)$[13] among other compounds[7,10,32] and has been successfully simulated. Isomer **7d** cannot form by direct oxidative addition of H_2 to **2d** since concerted cis addition as shown in eq 3 necessitates that one and only one hydride be trans to P. Instead, **7d** could form from **6d** or **5d** by either a cis reductive elimination/oxidative addition of HCN or an intramolecular rearrangement process. While isomers of the stereochemistry of **7d** are not observed for X = Br and I, the chloro isomer is seen by a similar AA'XX' hydride resonance at δ −6.81 to the extent of 1% of the equilibrium composition.

The oxidative addition of H_2 to Ir(CN)(CO)(dppe) (**1d**) thus follows the same pattern observed for the halide complexes, where addition via pathway iii in eq 3 is favored kinetically over pathway iv. The thermodynamics are different for the cyanide complex, however, as the kinetic product **5d** is now also the thermodynamically preferred isomer.

Reaction of D_2 with IrH(CO)(dppe). The complex IrH(CO)(dppe) (**1g**) has been proposed as an intermediate in the

Scheme I

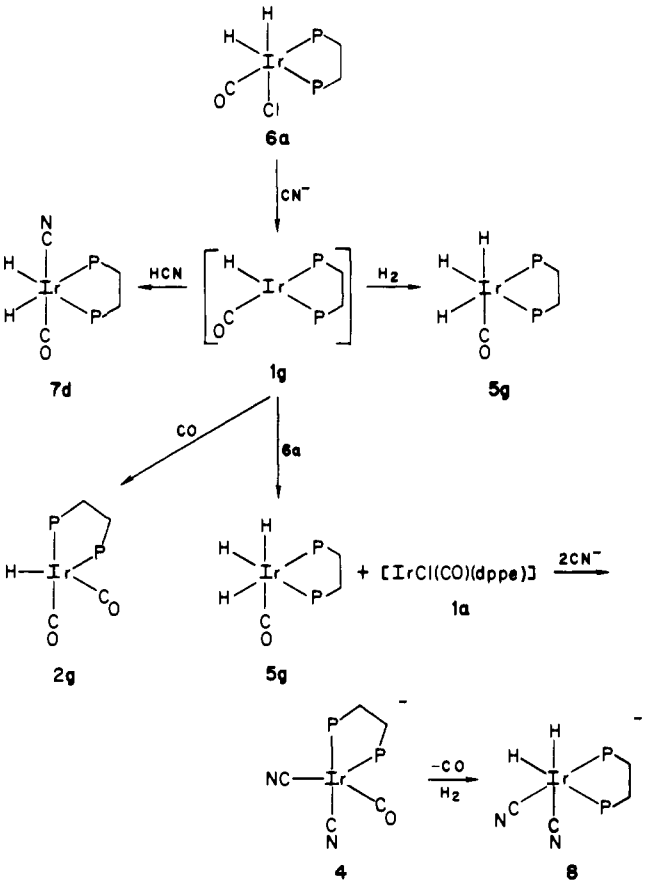

exchange reactions of $IrH(CO)_2(dppe)$ (**2g**) and $IrH_3(CO)(dppe)$ (**5g**).[13] In order to study the stereoselectivity of D_2 addition to **1g**, a method of generating **1g** under conditions where the expected product, **5g**-d_2, would be stable toward H_2 reductive elimination was devised based on dehydrohalogenation of **6a–c**. The viability

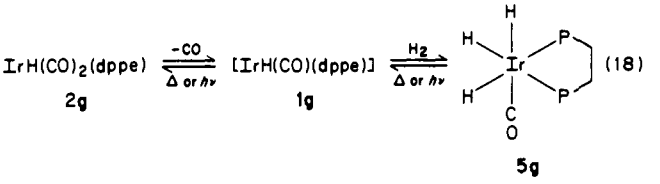

of this approach was discovered in an attempt to prepare **6d** by ligand exchange from the corresponding chloride complex, **6a**. The reaction of **6a** with PPN(CN) initially yielded three major products, **5g**, **4**, and **7d**, eq 19. Repeating the reaction under a

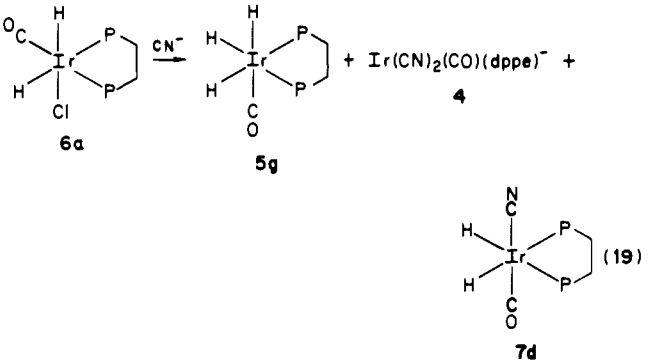

hydrogen atmosphere gave somewhat simpler results, eq 20. Complex **4** is observed as an intermediate in this reaction and disappears as **8** forms. The dihydride **8** can be prepared independently from the reaction of **4** and H_2 (see Table II for spectral data of **8**).[33] A small amount of **2g** (2%) was also observed in

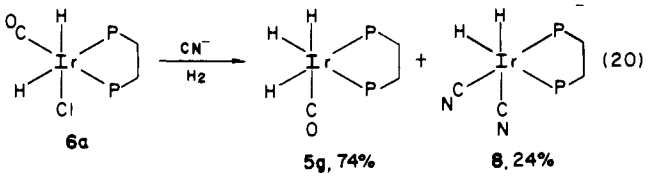

(20)

eq 20 as determined from ^{1}H NMR spectra. The observed products in eq 19 and 20 are explained by a mechanism involving dehydrohalogenation of **6a** by CN^- to form IrH(CO)(dppe) (**1g**) in situ and subsequent reactions as shown in Scheme I. The formation of the trihydride complex **5g** from **1g** in the presence of H_2, eq 20, occurs by H_2 oxidative addition. However, in the absence of H_2, eq 19, the formation of **5g** must occur via another path since the starting complex **6a** does not reductively eliminate H_2 on the time scale of the reaction. Instead, **5g** forms in eq 19 by direct attack of **1g** on **6a**, and the transfer of H_2 from the latter to the former is proposed to be effected by a hydride-bridged species such as **D**. Evidence for a very similar $Ir_2(\mu\text{-}H)_2$ species

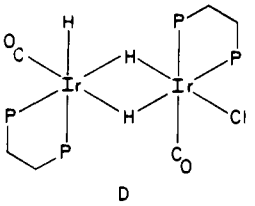

D

has been reported by Harrod.[8] The H_2 transfer from **6a** to **1g** also generates the four-coordinate Ir(I) chloro complex **1a** which rapidly reacts with CN^- to form **4** and ultimately **8** with any available H_2. The other two products, **7d** in eq 19 and **2g** in eq 20, are derived respectively from **1g** by oxidative addition of HCN formed in the initial reaction step[34] and by coordination of CO released from **4**, as shown in Scheme I. The scheme is in accord with the experimental observations which show that under vacuum, eq 19, the initial amounts of **5g** and **4** are nearly equal, whereas under H_2, eq 20, higher yields of **5g** are obtained at the expense of **4** + **8** and **7d**.

The notion that the reactions of Scheme I proceed by initial dehydrohalogenation of **6a–c** was supported by reacting **6b** with the base 1,8-diazabicyclo[5.4.0]undec-7-ene (DBU) under H_2 to yield the products shown in eq 21. The formation of **5b** occurs

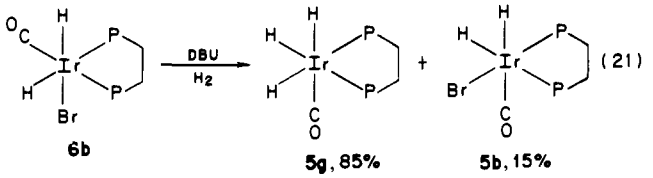

(21)

to the extent that the trihydride species **5g** forms by H_2 transfer from **6b** to **1g**. Complex **1b** will be generated in this process and oxidatively adds H_2 to yield the kinetic isomer **5b**. Dehydrohalogenation of the related complex $IrH_2Cl(CO)(PPh_3)_2$ has been reported previously, and in the presence of PPh_3 it yields $IrH(CO)(PPh_3)_3$.[35] The observation that IrH(CO)(dppe) (**1g**) can be generated by dehydrohalogenation under mild conditions makes possible a study of the stereochemistry of D_2 oxidative addition to **1g**. This was accomplished by reacting **6a** with CN^- under D_2, eq 22. The sample was prepared by first placing **6a** and 3 equiv of PPN(CN) in an NMR tube and then condensing in acetone

Table V. Deuterium Composition of $IrH_xD_{3-x}(CO)(dppe)$ (**5g**) Produced from the Reaction of $IrH_2Cl(CO)(dppe)$ (**6a**) with PPN(CN) under D_2

time, min	% D in **5g**	% scrambling in **5g**-d_2[a]
10	64	51
45	62	75
70	64	83
155	62	90
1560	68	98

[a] % scrambling = 3 × % of the isomer with H trans to CO. For a random deuterium distribution, the isomer ratio will be 1:2 and the percent scrambling 100%.

at −196 °C and flame-sealing the tube under 600 torr of D_2. When the acetone was half-thawed, the tube was shaken for 5 min to dissolve D_2 in solution. Since the dehydrohalogenation reaction occurs rapidly, even at −50 °C, it is essential that D_2 be dissolved at low temperature to serve as an efficient trap for **1g** in eq 22.

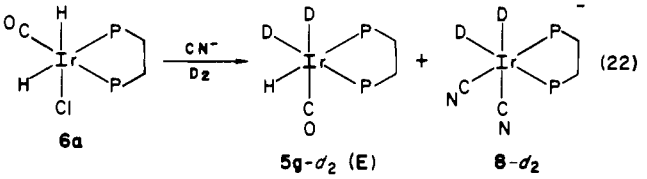

(22)

On the basis of ^{1}H NMR spectra in the phenyl region, the yield of products was 90% **5g** and 10% **8**. Several isotopomers are conceivable for **5g**, but ^{1}H NMR spectra indicate that isotopomer **E** shown in eq 22 predominates initially, and then it equilibrates with **F**, the other possible d_2 isomer, eq 23. According to Scheme

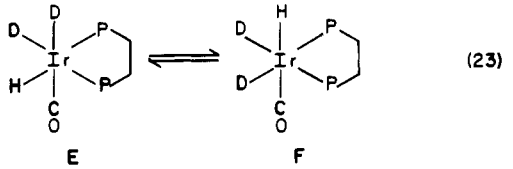

(23)

I, **5g**-d_0 should form to the same extent as **8** (10%) in eq 22. Assuming 10% **5g**-d_0, the relative amounts of **5g**-d_2 isotopomers were calculated (see Table V). The 63% observed deuterium incorporation into **5g** agrees well with the calculated value of 59% for an 8:1 mixture of **5g**-d_2 and **5g**-d_0. After 10 min there was a 5:1 ratio of isomers **E** and **F**, while equilibration to the statistical ratio of 2:1 occurred over several hours at 25 °C. Exchange with free D_2 does not occur during the H/D randomization, suggesting that the rearrangement occurs by an intramolecular process. Although oxidative addition of D_2 to **1g** could occur in two possible ways as shown in eq 24, no evidence has been found for the *mer* isomer **6g**. If indeed **6g**-d_2 had formed and then rapidly isomerized to **5g**-d_2, one should have seen at most a 2:1 ratio of isotopomers **E** and **F**. The fact that this was not the case allows us to conclude that D_2 adds stereoselectively to **1g** in the same direction observed for the corresponding halide and cyanide complexes (i.e., via pathway iii in eq 3).

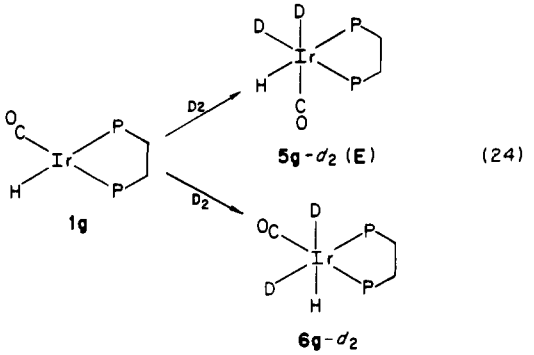

(24)

Reaction of H_2 with Ir(PPh$_3$)(CO)(dppe)$^+$. A solution of Ir-$(PPh_3)(CO)_2(dppe)^+$ (**2e**), prepared in situ as described earlier,

(32) Fryzuk, M. D.; MacNeil, P. A. *Organometallics* **1983**, *2*, 682–4.
(33) Complex **8** is characterized by its ^{1}H NMR spectrum which shows that one hydride is trans to phosphorus (J_p = 147 Hz) and the other hydride is trans to cyanide (δ −14.53).
(34) This result adds credence to the earlier suggestion that the equilibration of **7d** with **6d** or **5d** involves reductive elimination/oxidative addition of HCN.
(35) Harrod, J. F.; Gilson, D. F. R.; Charles, R. *Can. J. Chem.* **1969**, *47*, 1431–3.

was purged with H_2 for three min after which ^1H NMR spectra showed complete conversion to the dihydride **5e**, eq 25. The

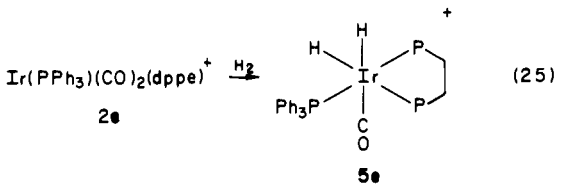

(25)

hydride resonances for **5e** occur at δ −10.05 (J_{PH} = 10.6, 18.0, and 114.7 Hz) for H trans to P(dppe) and δ −10.23 (J_{PH}(quartet) = 16 Hz) for H trans to CO (Table II). No isomerization of **5e** is observed at 25 °C, and **5e** is presumed to be the primary product formed via H_2 oxidative addition to the four-coordinate intermediate $Ir(PPh_3)(CO)(dppe)^+$ (**1e**). A more direct synthesis of **5e** is achieved by reacting **1b** and PPh_3 under H_2 in acetone solution. This reaction also appears to proceed with **1e** as an intermediate, and IR evidence for **1e** has been discussed earlier in the reaction of **1b** with PPh_3 (eq 7). Small amounts of the byproducts expected on the basis of eq 7, $IrH_2Br(CO)(PPh_3)_2$[22] and $IrH_2(dppe)_2^+$,[36] were also observed in the direct synthesis of **5e** from **1b**.

Comments on the Mechanism of H_2 Oxidative Addition and the Basis for Stereoselectivity. All of the compounds of the type IrX(CO)(dppe) (**1**) described in this study undergo stereoselective H_2 oxidative addition in which H_2 adds preferentially along the P–Ir–CO axis to yield the cis dihydride product in which one hydride is trans to P and the other is trans to CO (pathway iii in eq 3). This same stereochemistry of H_2 oxidative addition has also been reported by Bresadola et al. for complex **1** in which X is a carborane ligand.[18] Assuming H_2 oxidative addition is a concerted process, the results described here show that the approach of H_2 to **1** with its axis parallel to the P–Ir–CO axis, shown as **G**, is favored over the approach parallel to P–Ir–X, H, for every X ligand. The approach corresponding to **G** represents pathway iii in eq 3. For >99% stereoselectivity, the difference in activation energies between pathways iii and iv corresponding to **G** and H must be >2.7 kcal/mol.

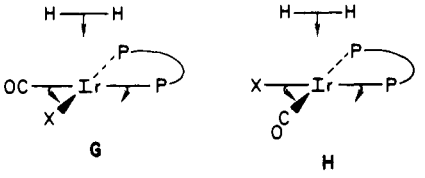

We now consider possible explanations for the observed stereoselectivity in H_2 oxidative addition to IrX(CO)(dppe). As outlined above, in these cis phosphine complexes, the observed stereochemical pathway for H_2 addition is determined solely by effects arising from the relative electronic and steric properties of the X and CO ligands. Since X ranges in size from PPh_3, I^-, and 7-Ph-1,7-$B_{10}C_2H_{10}^-$ to H^- and CN^- while maintaining the same stereoselectivity of H_2 addition to **1**, it is evident that the basis of the stereoselectivity observed here is electronic in origin and not steric. That we are looking at a kinetic phenomenon and not simply a consequence of the relative thermodynamic stability of the products (i.e., a reaction proceeding under product control) is established unambiguously in the cases where X = Cl, Br, and I. For these compounds, the isomer formed initially via pathway iii rearranges to the more stable isomer which would result from H_2 addition via pathway iv. For all X ligands in **1** the oxidative addition of H_2 is exothermic, suggesting that the transition state is achieved early in the reaction and thus appears more "reactant-like" as put forth by the Hammond postulate.[37]

As a basis for further discussion, we need to recall the important interactions in the H_2 oxidative addition reaction. These were illustrated as **A** and **B** above in which electron transfer from $\sigma^b(H_2)$ to an appropriate metal acceptor orbital such as p_z occurs with concomitant electron transfer from a metal donor orbital (d_{xz} or d_{yz}) to $\sigma^*(H_2)$. A recent paper by Saillard and Hoffmann[38] as well as studies by Sevin,[39] Dedieu,[40] Hay,[41] Morokuma,[42] and others[43] provide detailed theoretical analyses of the problem. In the H_2 oxidative addition, the interaction between H_2 and metal complex is synergic, but as Hoffmann points out, "the electron flow need not be balanced at every stage of the reaction".

Each of the two principal interactions, **A** and B, has been proposed as governing the early stages of the oxidative addition process. In addition, a four-electron repulsive interaction between $\sigma^b(H_2)$ and the filled metal d_{z^2} orbital has been invoked as a major contributor to the activation barrier for the H_2 oxidative addition.[40] In the present discussion, we focus on the relative importance of each of these interactions only as they relate to the observed stereoselectivity of H_2 addition.

Only the back-bonding or π-interaction **B** provides an obvious differentiation between the two orientations of approach, **G** and **H**. The σ interactions—bonding between $\sigma^b(H_2)$ and metal p_z, and repulsive between $\sigma^b(H_2)$ and d_{z^2}—cannot by themselves account for the preference of **G** over H. However, as the σ-bonding interaction **A** turns on during the oxidative addition process, one pair of trans ligands bends back to accommodate the incoming H_2 and facilitate the σ interaction further. There thus appear to be two factors which may be involved in establishing the stereoselectivity for the oxidative addition process—one concerns the back-bonding interaction B and the second regards the bending of trans ligands to facilitate the σ-bonding interaction of **A**.[44]

In the back-bonding interaction **B** involving complexes of type **1**, the d_π orbitals, d_{xz} and d_{yz}, are not degenerate, and their ability to interact with $\sigma^*(H_2)$ will not be equivalent. Since both overlap and energy match between d_π and $\sigma^*(H_2)$ determine the extent of interaction, each of these must be considered. Intuitively, we expect that the d_π orbital in H is higher in energy than the d_π orbital in **G** since the latter is stabilized by interaction with π^*-(CO). From an energetics standpoint, this would make the d_π orbital in H a better π-donor than the one in **G**. However, the experimentally observed result is that H_2 oxidative addition proceeds via **G**. The factor we propose to explain this result is based on overlap and comes into play at a very early stage in the oxidative addition process as H_2 approaches the metal complex. Specifically, we propose that H_2 approach via **G** is facilitated by increased overlap of $\sigma^*(H_2)$ with the metal-based d_π orbital through the involvement of π^*(CO) as shown in I.

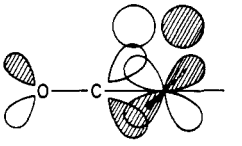

I

The second possible basis of the stereoselectivity of H_2 oxidative addition also merits consideration. In this proposal, the bending of trans ligands facilitates the σ interaction **A**, and the relative ease of bending determines the stereoselectivity. The logic here

(36) The ^1H NMR spectrum of this compound has been reported: Bedford, W. M.; Rouschias, G. *J. Chem. Soc., Dalton Trans.* **1974**, 2531–6.
(37) Hammond, G. S. *J. Am. Chem. Soc.* **1955**, *77*, 334–8.
(38) Saillard, J.-Y.; Hoffmann, R. *J. Am. Chem. Soc.* **1984**, *106*, 2006–26.
(39) Sevin, A. *Nouv. J. Chim.* **1981**, *5*, 233–41.
(40) Dedieu, A.; Strich, A. *Inorg. Chem.* **1979**, *18*, 2940–3.
(41) (a) Noell, J. O.; Hay, P. J. *J. Am. Chem. Soc.* **1982**, *104*, 4578–84. (b) Hay, P. J. *Chem. Phys. Lett.* **1984**, *103*, 466–9.
(42) Kitaura, K.; Obara, S.; Morokuma, K. *J. Am. Chem. Soc.* **1981**, *103*, 2891–2.
(43) (a) Shustorovich, E.; Baetzold, R. C.; Muetterties, E. L. *J. Phys. Chem.* **1983**, *87*, 1100–13. (b) Shustorovich, E. *Ibid.* **1983**, *87*, 14–7. (c) Hoffmann, R.; Chen, M. M.-L.; Thorn, D. L. *Inorg. Chem.* **1977**, *16*, 503–11. (d) Balazs, A. C.; Johnson, K. H.; Whitesides, G. M. *Ibid.* **1982**, *21*, 2162–74. (e) Tatsumi, K.; Hoffmann, R.; Yamamoto, A.; Stille, J. K. *Bull. Chem. Soc. Jpn.* **1981**, *54*, 1857–67.
(44) Harrod has proposed that the deformation of the square-planar complex is primarily responsible for the activation enthalpy in oxidative addition: Harrod, J. F.; Smith, C. A.; Than, K. A. *J. Am. Chem. Soc.* **1972**, *94*, 8321–5.

is similar to that applied to analyzing associative square-planar substitution reactions in terms of the relative stability of the developing trigonal bipyramid.[45] The approach **G** is favored over H because as the P–Ir–CO axis starts to bend in **G**, the greater π-acidity of CO serves to withdraw electron density from the metal center, and d_{z^2} in particular, reducing the repulsive interaction between $\sigma^b(H_2)$ and d_{z^2} as noted by Sevin.[39] While the bending also leads to destabilization of the d_π orbital in the plane of H_2 approach, possibly making it a better π donor from an energetics standpoint, it works against the overlap effect put forth as I in the previous paragraph.

The two effects discussed above to explain the observed stereoselectivity thus appear to be in conflict, and at this time it is not possible to determine which effect controls the stereoselectivity. Examination of concerted stereoselective oxidative additions using other substrates, such as R_3SiH and HX, and their relevance in establishing the basis of the observed stereoselectivity are presented in another paper.

Evidence for ligand electronic effects controlling the direction of H_2 oxidative addition has also been reported recently by Crabtree and Uriarte,[46] who studied the reaction of H_2 with Ir(cyclooctadiene)$(Ph_2POCH_2CH_2PPh_2)^+$, eq 26. Only the

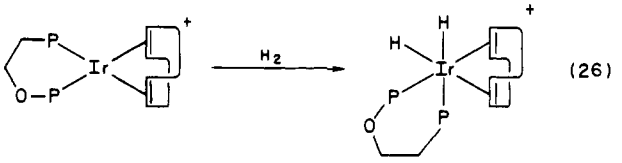

(26)

dihydride shown was observed, and the result was analyzed in terms of the relative stability of 5-coordinate trigonal-bipyramidal H_2 adducts, **J** and **K**, in which H_2 acts as a $2e^-$ donor ligand for the two different orientations of approach. On the basis of the observed stereoselectivity, it was proposed that **J** is preferred over **K** since this places H_2 in the equatorial plane with the phosphorus ligand which is the better donor and poorer π-acceptor, facilitating the back-bonding interaction into $\sigma^*(H_2)$.

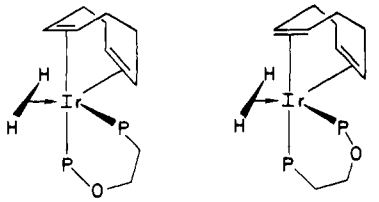

This proposal contradicts the analysis given above for the relative preference of bending trans ligands since the better π-acid ligand occupies an axial rather than an equatorial position in **J**, but it can be accommodated by the back-bonding argument if one assumes that the 3d acceptor orbitals on the phosphine donor are more spatially extended than the same orbitals on the phosphinite donor.

Concluding Remarks. In this study we have shown that H_2 oxidatively adds to IrX(CO)(dppe) in a stereoselective way which is controlled by electronic factors of the CO and X ligands. For the cases of X = Cl, Br, and I, the stereoselectivity is shown to be of kinetic origin with subsequent conversion of the initially formed isomer to the more stable cis dihydride isomer. For all X the same stereoselectivity is observed corresponding to pathway iii of eq 3. While it is clear that the basis of the stereoselectivity is electronic, the specific controlling factor is less well defined, and may relate to enhanced overlap in the π-back-bonding interaction between metal d and $\sigma^*(H_2)$ at an early stage of the oxidative addition process, or to preferred bending of one set of trans ligands as the oxidative addition reaction proceeds.

(45) (a) See discussion and references in: Huheey, J. E. "Inorganic Chemistry", 2nd ed.; Harper & Row: New York, 1978; p 496. (b) Reference 1c, p 1201.

(46) Crabtree, R. H.; Uriarte, R. J. *Inorg. Chem.* **1983**, *22*, 4152–4.

Experimental Section

Materials. The following reagents were used as received: $AgNO_3$ (Fisher A.C.S.), tetra-*n*-butylammonium (TBA) bromide, 1,8-diazabicyclo[5.4.0]undec-7-ene (DBU), $AgBF_4$ (Aldrich), H_2 (Air Products 99.9%), D_2 (Matheson C.P., 99.5%), and CO (Air Products C.P., 99.3%). Triphenylphosphine (Aldrich) and 1,2-bis(diphenylphosphino)ethane (dppe) (Alfa) were recrystallized from hot ethanol. Bis(triphenylphosphine)iminium (PPN) cyanide was prepared by the literature method from PPNCl[47] and KCN (Mallinckrodt) in methanol.[48] Solvents are reagent grade except benzene-d_6 (Aldrich Gold Label, 99.5% D, distilled from Na/benzophenone), acetone-d_6 (Aldrich Gold Label, 99.5% D, distilled from Linde 4A molecular sieves), and THF (distilled from Na/benzophenone).

Preparation of Complexes. The complexes IrCl(CO)(dppe) (**1a**),[12] IrBr(CO)(dppe) (**1b**),[12] and IrI(CO)(dppe) (**1c**)[13] were prepared from $PPN[IrCl_2(CO)_2]$,[49] $TBA[IrBr_2(CO)_2]$,[50] and $TBA[IrI_2(CO)_2]$,[49] respectively, by the procedures reported previously. The side product $[Ir(CO)(dppe)_2][IrBr_2(CO)_2]$ was isolated as yellow crystals by addition of ethanol to the filtrate obtained in the synthesis of **1b** and was characterized by IR (KBr pellet) stretches at 2049 (s), 1962 (s, br), and 1941 (s) cm^{-1} (cf. 2051, 1963, 1935 (sh) cm^{-1} reported for the chloro analogue[15]).

Benchtop reactions were performed under a nitrogen atmosphere (unless otherwise indicated) with a Schlenk-type vacuum line. The general procedure for preparing sealed-tube samples for ^1H NMR experiments involved placing ca. 6 mg of Ir complex in a 5-mm NMR tube attached to a 14/20 glass joint. On a high-vacuum line 0.5 mL of solvent was condensed into the tube at −196 °C and, if desired, the sample pressurized with 600 torr of H_2 prior to flame sealing. All of the Ir(I) complexes are air sensitive in solution, but as solids they can be handled for brief periods of time in air.

Physical Measurements. ^1H and ^{31}P NMR spectra were recorded on a Bruker WH-400 spectrometer at 400.13 and 162.00 MHz, respectively. Chemical shifts are reported in ppm downfield from external references (Me_4Si for ^1H and 85% H_3PO_4 for ^{31}P) but were usually calculated from residual ^1H solvent resonances (acetone-d_5 δ_H 2.04, benzene-d_5 δ_H 7.15). The temperature for kinetic NMR experiments was regulated by a Bruker BVT-1000 temperature control unit (±0.1 °C). IR spectra were recorded on a Perkin-Elmer 467 spectrophotometer.

Reaction of IrI(CO)(dppe) (1c) or IrBr(CO)(dppe) (1b) with PPN(CN). The reaction of **1c** or **1b** with PPN(CN) has been followed independently by IR, ^1H NMR, and ^{31}P NMR spectroscopies. In the IR experiment, THF was added to equimolar amounts of **1c** (ν_{CO} 1990 cm^{-1}) and PPN(CN). The mixture was stirred for 10 min, yielding an orange solution with IR stretches at 2120 (w), 1997 (s), and 1957 (m) cm^{-1} and a cream precipitate. The peaks at 2120 and 1997 cm^{-1} are assigned to Ir(CN)(CO)(dppe) (**1d**). The precipitate was collected by removing the solution via cannula and washing with benzene. The IR spectrum (KBr pellet) of the precipitate matched that of PPNI. Under a CO atmosphere the above orange solution turned pale yellow with IR stretches at 2142 (w), 2005 (m), and 1959 (s) cm^{-1} assigned to $Ir(CN)(CO)_2(dppe)$ (**2d**). Addition of heptane afforded a pale yellow precipitate which was recrystallized from benzene–heptane under CO to give pure **2d**. Anal. Calcd for $IrC_{29}H_{24}NO_2P_2$: C, 51.78; H, 3.60; N, 2.08. Found: C, 51.94; H, 3.77; N, 1.88 (Galbraith Laboratories).

In acetone solution the results are completely analogous except that the solution remains homogeneous throughout the reaction. If two or more equivalents of PPN(CN) are used, a yellow solution is obtained with IR stretches at 2094 (w) and 1900 (s, br) cm^{-1}, assigned to $Ir(CN)_2(CO)(dppe)^-$ (**4**). ^1H and $^{31}P\{^1H\}$ NMR data for **1d**, **2d**, and **4** in acetone solution are presented in Table I.

Reaction of 1b with PPh_3. One equivalent of PPh_3 was added to an acetone solution of **1b** and the reaction monitored by IR spectroscopy. After 4 min three IR peaks were observed in the terminal CO region: 2008 (w), 1963 (s), 1915 (s) cm^{-1}. The peaks at 2008 and 1915 cm^{-1} disappear over a period of 20 min as a peak grows in at 1940 (s) cm^{-1} assigned to $Ir(CO)(dppe)_2^+$. At this time orange-yellow crystals begin to form, and they are identified as $IrBr(CO)(PPh_3)_2$ by IR (ν_{CO} 1963 cm^{-1}) comparison to an authentic sample.

Reaction of 1b with $AgNO_3$ and PPh_3. Acetone was added to equimolar amounts of **1b** and $AgNO_3$ and the mixture stirred for 15 minutes under an atmosphere of CO. One equivalent of PPh_3 was then added and the product characterized as $Ir(PPh_3)(CO)_2(dppe)^+$ (2e) by the IR and ^1H NMR spectral data in Table I.

(47) Ruff, J. K.; Schlientz, W. J. *Inorg. Synth.* **1974**, *15*, 84.

(48) Martinsen, A.; Songstad, J. *Acta Chem. Scand. Ser. A* **1977**, *A31*, 645–50.

(49) Forster, D. *Inorg. Nucl. Chem. Lett.* **1969**, *5*, 433–6.

(50) Cleare, M. J.; Griffith, W. P. *J. Chem. Soc. A* **1970**, 2788–94.

Reaction of 1a–c with H_2. These reactions were generally carried out in sealed NMR tubes as described above. In synthetic scale reactions benzene solutions of **1a–c** were stirred overnight under an H_2 atmosphere. The isomerization reaction **5** → **6** was monitored by IR spectroscopy. For the case of bromide, the IR peaks at 2105 (m, ν_{Ir-H}) and 2007 (m, ν_{CO}) cm^{-1} for **5b** are replaced by corresponding peaks for **6b** at 2175 (w, ν_{Ir-H}) and 2042 (s, ν_{CO}) cm^{-1}. The chloride complex **6a** is nearly insoluble in benzene and precipitates as colorless crystals during the reaction. The bromide and iodide analogues **6b** and **6c** are precipitated by addition of ethanol, collected by filtration, and washed with ethanol and pentane.

Reaction of 5b with D_2, CO, and PPN(CN). For the D_2 and CO experiments 1–5 mg of **1b** was placed in an NMR tube and 0.5 mL of benzene or acetone was condensed into the tube at −196 °C on a high-vacuum line. The sample was exposed to 600 torr of H_2 and then thawed and shaken up briefly to allow reaction with H_2. After freezing the solution with liquid nitrogen the sample was evacuated and then charged with 600 torr of D_2 or CO. After flame-sealing, the sample was thawed, shaken vigorously for 1 min, and then examined by ^1H NMR spectroscopy.

The PPN(CN) experiment in acetone was set up similarly except that PPN(CN) was placed in a sidearm between the NMR tube and the 14/20 glass joint. After allowing for the reaction of **1b** with H_2 as above, the solution was tipped into the sidearm containing PPN(CN) and shaken for 2 min to give a homogeneous solution. The solution was then tipped back into the NMR tube and frozen, and the tube was flame-sealed.

Reaction of 6c or 6b with CO, D_2, and PPh_3. These experiments were performed in sealed-tube benzene solutions according to the general procedure outlined above with 4 mg of iridium complex. The progress of the reaction was monitored by ^1H NMR spectroscopy.

Reaction of the Cyanide Complexes 1d, 2d, and 4 with H_2. The reaction of **2d** with H_2 was studied by ^1H NMR spectroscopy with a sealed-tube sample prepared by the usual method. Identical results were obtained from the reaction of H_2 with **1d** prepared in situ from **1b** and 1.0 equiv of PPN(CN). In this case acetone was condensed at −196 °C into an NMR tube containing **1b** and PPN(CN). After warming to room temperature, the sample was shaken for 1 min to give a homogeneous orange solution and then frozen and sealed under 600 torr of H_2. The major product from these reactions, **5d**, was isolated by first removing acetone solvent under vacuum, stirring the residue with toluene to separate out insoluble PPN salts, and finally treating the toluene solution with heptane to precipitate the product.

The reaction of **4** with H_2 was followed by ^1H NMR spectroscopy with a sealed-tube sample prepared by the procedure described above for the reaction of **1d** and H_2. Complex **4** was prepared in situ from **1b** and 2.5 equiv of PPN(CN). After thawing, the initial ^1H NMR spectrum showed peaks for **4** as the only iridium species. Over the course of several hours the yellow solution gradually turns colorless as conversion to **8** occurs. Complex **8** was isolated by removing the solvent under vacuum, dissolving the residue in CH_2Cl_2, and then precipitating the product with heptane.

Reaction of 6a with PPN(CN) under Vacuum, H_2, and D_2. These reactions were all performed in sealed NMR tubes and monitored by ^1H NMR spectroscopy. For the reaction under vacuum, 2.9 mg of **6a** and 5.3 mg of PPN(CN) (2.1 equiv) were placed in an NMR tube, 0.5 mL of acetone was condensed in at −196 °C, and the tube was flame-sealed. After warming to room temperature the tube was shaken for 10 min to give a homogeneous yellow solution. For the reaction under H_2 the same procedure was used except that the tube was sealed under 600 torr of H_2. In the case of D_2, 2 mg of crystalline **6a** was used along with 3 equiv of PPN(CN). When the acetone was half-thawed the tube was shaken for 5 min to give a nearly homogeneous colorless solution.

Reaction of 6b with DBU under H_2. A solution of 2.7 mg of **6b** in 0.5 mL of acetone in a septum-capped NMR tube was purged with H_2 and then 3 μL of DBU (5 equiv) was added. After 10 min the solution was analyzed by ^1H NMR spectroscopy.

Reaction of 2e with H_2. An acetone solution of **2e** prepared in situ as described above was transferred to a septum-capped nitrogen-purged NMR tube and then purged with H_2 for 1 min. A ^1H NMR spectrum indicated 70% conversion of **2e** to **5e**. An additional 2-min H_2 purge resulted in complete conversion to **5e**. Complex **5e** was precipitated as the nitrate salt by addition of heptane.

Reaction of 1b with PPh_3 under H_2. Compound 1b (5 mg) and PPh_3 (2 mg, 1.2 equiv) were placed in an NMR tube and the sample made up with benzene or acetone solvent according to the usual sealed-tube procedure. After thawing, the sample was shaken for 30 s to give a colorless solution. For the benzene solution the ^1H NMR spectrum taken 3 min after thawing showed peaks for three hydride species (relative integrated amount): **5e** (77%), $IrH_2Br(CO)(PPh_3)_2$[22] (8%, δ_H −7.35 (dt, J_P = 13.1 Hz, J_H = 4.3 Hz), −16.63 (dt, J_P = 9.5 Hz, J_H = 4.3 Hz)), and **5b** (15%). After 42 min two hydride species were evident: **5e** (91%) and $IrH_2Br(CO)(PPh_3)_2$ (9%). A third hydride species eventually appeared over the course of several hours to the extent of 4% and was identified as $IrH_2(dppe)_2^+$ (δ_H −11.53 (~dq, J_P(cis) ≈ 15 Hz, J_P(trans) = 111 Hz; cf. literature values of δ −11.7 with J_P(trans) = 110 Hz for acetonitrile solution)[36]). In acetone solution the same three dihydride products were observed but the amount of the side products, $IrH_2Br(CO)(PPh_3)_2$ and $IrH_2(dppe)_2^+$, is reduced.

Table VI. Summary of Crystallographic Data

compd	$IrH_2Br(CO)(dppe)$ (**6b**)
formula	$C_{27}H_{26}OP_2BrIr$
fw	700.58
crystal dimensions	0.4 × 0.3 × 0.25 mm
space group	$P2_12_12_1$
cell parameters	
a, Å	12.291 (3)
b, Å	17.349 (4)
c, Å	12.189 (3)
V, Å^3	2599
Z	4
d(calcd), g/cm^3	1.790
abs coeff (μ), cm^{-1}	67.8
max, min, av transmission factors	1.00, 0.78, 0.90
systematic absences	$h00$, h odd; $0k0$, k odd; $00l$, l odd
data collected	$\pm h,+k,+l$
diffractometer	Enraf–Nonius CAD4
temp, °C	23
radiation	Mo K$\bar{\alpha}$ (λ = 0.7107 Å, graphite monochromator)
scan mode	ω–2θ
takeoff angle, deg	2.6
ω scan angle	1.00° + 0.35 tan θ
scan speed, deg/min	4.0–20.1
total background time	$^1/_2$ peak scan time
2θ range, deg	4–46
reflcns measured	3952
unique data after av equiv reflcns	3624
reflcns used	2979 ($I > 3\sigma(I)$)
no. of parameters varied	289
p	0.04
R	0.035
R_w	0.042
GOF	1.40

X-ray Structural Determination of $IrH_2Br(CO)(dppe)$ (6b). Data Collection and Reduction. Colorless crystals of **6b** were obtained from a sealed NMR tube sample which initially contained **1b** and 1.5 equiv of pyridine in benzene under 600 torr of H_2. The presence of pyridine in the sample had no effect on the reaction chemistry, according to ^1H NMR spectra which showed the initial formation of **5b** and subsequent conversion to **6b**. A crystal was affixed to the end of a glass fiber with melted shellac and mounted on the kappa goniometer. The orthorhombic space group $P2_12_12_1$ was determined by use of the Enraf-Nonius CAD4-SDP peak search, centering, and indexing programs.[51] Table VI contains a summary of crystallographic data. Background counts were measured by extending the indicated scan range by 25% on both sides of the peak. The intensities of three standard reflections were monitored every 2 h of X-ray exposure, and the average total intensity variation during 30 h was ±1.5%. Orientation control was checked every 200 reflections by the same three standard reflections. The data were corrected for Lorentz, polarization, and background effects. A semi-empirical absorption correction was applied to the data based on a transmission curve determined by ψ-scan data. Of the 3952 reflections meaured, 3288 are unique and the remaining equivalent reflections were

(51) Calculations were carried out on the Molecular Structure Corporation Texray 230 computer system (PDP 11/23 processor) with the Enraf–Nonius CAD4 and SDP-Plus programs. For a description of the crystallographic computing package see: Frenz, B. A. In "Computing in Crystallography"; Shenk, H., Olthof-Hazekamp, R., van Konigsveld, H., Bassi, G. C. Eds.; Delft University Press: Delft, Holland, 1978; pp 64–71. See also: "CAD4 Operators Manual"; Enraf–Nonius Delft: Delft, Holland, 1982; "Structure Determination Package-User's Guide"; B. A. Frenz & Associates: College Station, Texas; and Enraf–Nonius: Delft, Holland, 1982. The function minimized in least-squares refinement is $\sum w(|F_o| - |F|)^2$, where $w = 1/[\sigma(F_o)]^2$. The residuals are defined as $R = (\sum||F_o| - |F_o||)/\sum|F_o|$ and $R_w = [\sum w(|F_o| - |F_c|)^2/\sum wF_o^2]^{1/2}$. The error in an observation of unit weight (GOF) is $[\sum w(|F_o| - |F_c|)^2/(NO-NV)]^{1/2}$, where NO is the number of observations (reflections) and NV is the number of variables. The perspective thermal ellipsoid plot was done with the SDP version of C. K. Johnson's ORTEP plotting program.

averaged, giving an agreement factor of 0.024 on F_o for the averaged observed reflections.

Solution and Refinement of the Structure. The structure was solved by conventional heavy-atom techniques.[51] The positions of the iridium and bromine atoms were determined from a Patterson synthesis. All other non-hydrogen atoms were located from difference Fourier maps following full-matrix least-squares refinement of previously located atoms. Atomic scattering factors were taken from the usual tabulations and the effects of anomalous dispersion were included.[52] After anisotropic refinement of the non-hydrogen atoms, the dppe hydrogen atom positions were calculated (C-H distance 0.95 Å) and included in structure factor calculations but were not refined (fixed isotropic thermal parameters were 5.0 Å^2 for CH_2 hydrogens and 6.5 Å^2 for phenyl hydrogens). Final least-squares refinements established the correct enantiomer for the structure in $P2_12_12_1$ and led to the R values and esd in an observation of unit weight given in Table VI. The final difference Fourier showed only one peak with electron density greater than 25% of the height of a typical C atom. This peak was located ca. 2.3 Å from Ir with a height of 60% of a typical C atom. The location of this peak which did not refine successfully suggests that if it is not an artifact, it may be due to co-crystallization of <1% of the kinetic isomer **5b** with crystal packing determined by the Ir(dppe) part of the complex.

Tables III and IV in the text contain final positional parameters and selected bond distances and angles. Calculated hydrogen atom positions, refined anisotropic thermal parameters, and a listing of observed and calculated structure factor amplitudes are available as supplementary material.

(52) Cromer, D. T.; Waber, J. T. "International Tables for X-ray Crystallography"; Ibers, J. A., Hamilton, W. C., Eds.; Kynoch Press: Birmingham, England, 1974; Vol. IV, Table 2.2B. Cromer, D. T. *Ibid.*, Table 2.3.1.

Acknowledgment. We thank the National Science Foundation (Grant CHE83-08064) and the Office of Naval Research for support of this research. We also thank Johnson Matthey Co. Inc. for a generous loan of iridium salts. Early efforts in this study by Dr. Barbara J. Fisher are greatly appreciated. Finally, we thank Professor Peter Wolczanski of Cornell for helpful and stimulating comments.

Supplementary Material Available: Listings of anisotropic thermal parameters (Table VII), bond lengths and angles within phenyl groups (Table VIII), calculated hydrogen atom positions (Table IX), and observed and calculated structure factors (Table X (34 pages). Ordering information is given on any current masthead page.

Study of the Reactions of Substituted Allenes with Tris(triphenylphosphine)nickel(0). An Analysis of the Factors Affecting the Regio- and Stereochemistry of π-Complex Formation and Coupling To Form Nickelacyclopentane Complexes

Daniel J. Pasto,* Nai-Zhong Huang, and Charles W. Eigenbrot

Contribution from the Department of Chemistry and the Molecular Structure Facility, University of Notre Dame, Notre Dame, Indiana 46556. *Received December 5, 1984*

Abstract: The reactions of ethylallene (ETA), *tert*-butylallene (TBA), phenylallene (PHA), cyanoallene (CYA), and methoxyallene (MEA) with tris(triphenylphosphine)nickel(0) [$(TPP)_3Ni$] have been investigated and compared with the reaction of dimethylallene (DMA) with $(TPP)_3Ni$ reported earlier. At low temperatures (<-70 °C) ETA, TBA, and DMA reversibly form mono- and bis-allene π-complexes which can be detected by NMR. π-Complex formation involves predominantly the least substituted double bond. DMA displaces ETA and TBA, while MEA in turn displaces DMA from the π-complexes. PHA and CYA undergo immediate coupling at low temperatures (<-70 °C), and the relative stabilities and structures of their π-complexes could not be determined. The relative stabilities and structures of the π-complexes are discussed in terms of steric and electronic effects. The cis bis-π-complexes undergo coupling to form nickelacyclopentane σ-complexes: the relative reactivity sequence being CYA > PHA > MEA $\gg$ DMA > ETA > TBA. Evidence for a competitive electron-transfer process with CYA is presented. The structures of the intermediate substituted nickelacyclopentane complexes are inferred from the structures of the hydrocarbon products formed in reductive-elimination and hydrogen-migration, reductive-elimination reactions and from the structures of the ketonic products formed on reaction with carbon monoxide. Specific π-π, π-σ, and σ-σ modes of coupling in syn and anti conformations of the bis-π-complexes have been identified. The regio- and stereochemistry of formation of the nickelacyclopentane σ-complexes are discussed in terms of steric and electronic (orbital energy and AO coefficients) effects in the rate-determining transition state for σ-complex formation.

Our discovery that the formation of substituted allenes in the reactions of Grignard reagents with propargyl halides is catalyzed by salts of iron, cobalt, nickel and copper[1] and the reductive cyclization of propargyl chlorides with tris(triphenylphosphine)-nickel(0) [$(TPP)_3Ni$] to form 3,4-bis(alkylidene)cyclobutenes[2] has led us to study in detail the reactions of allenyl and propargyl systems with low valence state transition metal complexes. Recent studies have focused on the reactions of substituted allenes with Ni(0) complexes. Although several reports had appeared describing the reactions of allene with Ni(0) complexes,[3] relatively few investigations had been carried out with substituted allenes. It had been observed that dimethylallene (DMA) was converted to the dimeric-triene **1** in the presence of $[(o\text{-}CH_3C_6H_4O)_3P]_3Ni$ and that 1,2-cyclooctadiene forms a π-complex with the same

(1) Pasto, D. J.; Chou, S.-K.; Waterhouse, A.; Shultz, R. H.; Hennion, G. F. *J. Org. Chem.* **1978**, *43*, 1385.
(2) Pasto, D. J.; Mitra, D. K. *J. Org. Chem.* **1982**, *47*, 1381.

(3) Otsuka, S.; Mori, K.; Imaizumi, F. *J. Am. Chem. Soc.* **1965**, *87*, 3017. Otsuka, S.; Mori, K.; Suminoe, T.; Imaizumi, F. *Eur. Polym. J.* **1967**, *3*, 73. Hoover, F. W.; Lindsey, R. V., Jr. *J. Org. Chem.* **1969**, *34*, 3051. Otsuka, S.; Nakamura, A.; Tani, K.; Ueda, S. *Tetrahedron Lett.* **1969**, 297. DePasquale, R. J. *J. Organomet. Chem.* **1971**, *32*, 381. Otsuka, S.; Tani, K.; Yamagata, T. *J. Chem. Soc., Dalton Trans.* **1973**, 2491.

0002-7863/85/1507-3160$01.50/0